2006

Fabrication of Polymer Based Optical Devices for Communication and Sensing

Sandhya Pochiraju
University of Kentucky, sandhya@uky.edu

Abstract of Thesis

Fabrication of Polymer Based Optical Devices for Communication and Sensing

Polymer waveguides present a potentially low cost alternative to electronics in communication systems. Polymers offer relatively straightforward and economical fabrication when compared to conventional materials. In this study, a fabrication process for Bragg gratings in polymer waveguides was developed. Waveguides were designed using finite-element analysis, patterned via e-beam lithography, and a detailed fabrication method was developed.

Surface-Plasmon Resonance (SPR) is a widely accepted method for biological and chemical sensing. Measurement of bulk refractive index changes and specific surface binding is a crucial part in any biosensing. Design and fabrication of a novel self-referencing SPR sensor is described and its functionality is tested.

KEYWORDS: Surface-plasmon, Teflon AF-1600, Bragg grating, SPR, Femlab, Polymer Waveguide, PMMA.

Sandhya Pochiraju

Author's Signature

December 2, 2005

Date

Fabrication of Polymer Based Optical Devices for Communication and Sensing

By

Sandhya Pochiraju

Dr Todd Hastings
Director of Thesis

Dr YuMing Zhang
Director of Graduate Studies

December 2, 2005
Date

RULES FOR THE USE OF THESES

Unpublished theses submitted for the Master's degree and deposited in the University of Kentucky Library are as a rule open for inspection, but are to be used only with due regard to the rights of the authors. Bibliographical references may be noted, but quotations or summaries of parts may be published only with the permission of the author, and with the usual scholarly acknowledgments.

Extensive copying or publication of the thesis in whole or in part also requires the consent of the Dean of the Graduate School of the University of Kentucky.

A library that borrows this thesis for use by its patrons is expected to secure the signature of each user.

Name Date

THESIS

Sandhya Pochiraju

The Graduate School
University of Kentucky
2005

Fabrication of Polymer Based Optical Devices for Communication and Sensing

---

THESIS

A thesis submitted in partial fulfillment of the requirements for the degree of Master of Science in the College of Engineering at the University of Kentucky

By

Sandhya Pochiraju

Lexington, KY

Director: Dr Todd Hastings, Assistant Professor of Electrical Engineering

Lexington, KY

2005

MASTERS THESIS RELEASE

Sandhya Pochiraju

December 2, 2005

ACKNOWLEDGEMENTS

Dr.Todd Hastings (Advisor)

Mr. George Spiggle

Committee Members

- Dr. Zhi Chen
- Dr. Cai - Cheng Lu

Fellow Lab Members

- Adam W Chamberlain
- Babitha Bommalakunta
- Pang Leen Ong
- Raghunandan Donipudi
- Vashista de Silva

TABLE OF CONTENTS

LIST OF TABLES AND PLOTS

LIST OF FIGURES

Chapter 1

INTRODUCTION

1.1 Background

In 1880 Alexander Graham Bell invented the photo phone. He tried to transmit sound waves of human speech by focusing a beam of sunlight on a thin mirror. The sound waves caused the mirror to vibrate which caused corresponding variation in the energy transmitted to the light detector [1]. This in turn varied the resistance of the detector which caused the current in the telephone to vary. Bell could send voice signals 700 feet using this setup.

In the present day optical systems provide much higher bandwidth and much longer distance communications. Photonic systems generally offer very large information capacity (bandwidth) [2]. Apart from this they offer low transmission losses, less heat generation, immunity to cross talk and immunity to electromagnetic interference when compared to electric transmission systems.

There are two kinds of broad band communications – free space optics and guided wave optics. The former one can be realized over a few kilometer distances where source and destination are visible to each other. In this case atmosphere is the transmission medium. Guided wave optical communication, and specifically optical fiber communication is more practical and useful for current communication needs. Guided wave optics applies the principle of total internal reflection to confine the light inside the core of the waveguide. More on this will be dealt with further in later chapters.

Apart from communications, photonics also play a crucial role in biological and chemical sensing. During the last two decades there has been great research activities

aimed towards development of optical sensors. Among other methods of optical sensing like ellipsometry, surface plasmon resonance (SPR) is gaining lot of attention and SPR is increasingly being used for the sensing purposes. In 1982, Nylander and Liedberg demonstrated the SPR based sensors for gas detection. Since then most work has focused on exploiting SPR for optical bio sensing. The later chapters cover more about SPR sensor operation and fabrication.

This thesis work is aimed at fabricating and characterizing integrated polymer waveguides for Bragg gratings based filters and SPR sensors. A detailed fabrication procedure has been described for the both. However due to various obstructions in finding the right materials and problems with the working of related equipment only SPR sensors could be practically realized and characterized. However a detailed methodology for fabrication of waveguides and their modeling has been documented to provide a starting point for future work.

1.2 Why Polymer Waveguides and Why Teflon

Though much progress has been achieved in the design and production of integrated dielectric waveguides (DWG), the right material for these structures is still an unanswered question. Indium Phosphide (InP) based waveguides are often a popular choice. But the processing involved with it is highly complex and the materials are extremely expensive. Among other contestants, the one drawing lot of attention is the class of polymers. Numerous polymer based waveguide devices have been made in the past, and great progress is being made to develop waveguides suitable for communication and sensing purposes. For communications wavelengths near 1550nm polymer

waveguides are attractive because they are relatively simple to process, cost effective and exhibit low optical loss. Apart from this they offer a possibility to fabricate dense integrated circuits, suitable for present requirements. There is a possibility of achieving high contrast index, which makes the device smaller and reduces the bending losses.

In 1994, Anadi Mukherjee [3] et al. fabricated channel waveguide with PMMA (n = 1.47) as core and SiO_2 (n = 1.45) as cladding. W.H.Wang et al. [4] successfully fabricated fiber Bragg grating waveguides with Novolak (ENR) resin polymer (from MicroChem, n = 1.57) as core and SiO_2 as cladding. In 2000, Y.G.Zhao [5] et al. reported channel waveguide with PMMA as core and Cytop ((Asahi Glass Company) as cladding. Cytop (n = 1.36) is similar to Teflon AF-1600 in terms of refractive index. Teflon is one of the polymers with a very low refractive index of 1.3036. Our design of devices using Teflon AF-1600 as cladding offers high contrast in refractive indices of core and cladding. The light signal will be confined more strongly in the core when the difference between refractive indices of core and cladding is greater. The combination of PMMA and Teflon AF-1600 offers higher refractive index contrast than any one of the previous polymer waveguide devices. In addition, the use of Teflon is particularly important for bio-chemical sensors working in solutions. In this case the refractive index of the cladding must closely match the refractive index of the sensor.

1.3 Bragg Gratings in Optical Waveguides

Waveguides used for optical communication are made of transparent dielectrics. The core of the waveguide is made of a higher refractive index material and is surrounded by a cladding of lower refractive index material. The principle of total

internal reflection causes the optical wave to be confined in the core of the waveguide. This difference in the refractive indices causes the wave to be confined inside the core.

The core of typical optical waveguides is of uniform refractive index through out its length. However, it is possible that to vary the refractive index or the geometric dimensions of the core periodically along its length. Such structures are called gratings. A particular type of grating, the Bragg gratings, reflects light over a narrow wavelength range and transmits the other wavelengths. The wave length which is reflected back depends on the period of variation of refractive index and the effective index of the waveguide.

$$\lambda_b = 2\Lambda\eta_{eff}$$

Where λ_b = wavelength of reflected light

Λ = grating period

η_{eff} = effective refractive index.

Each change in refractive index or waveguide dimensions reflects a small amount of light. If the wavelength of light satisfies the above equation then the reflections from each high refractive index zone interfere constructively and cause complete reflection of that particular wavelength. The wavelengths not fitting the above equation are transmitted through the grating as the reflections in this case interfere destructively and are cancelled.

The following figure shows a schematic representation of a Bragg gratings based waveguide.

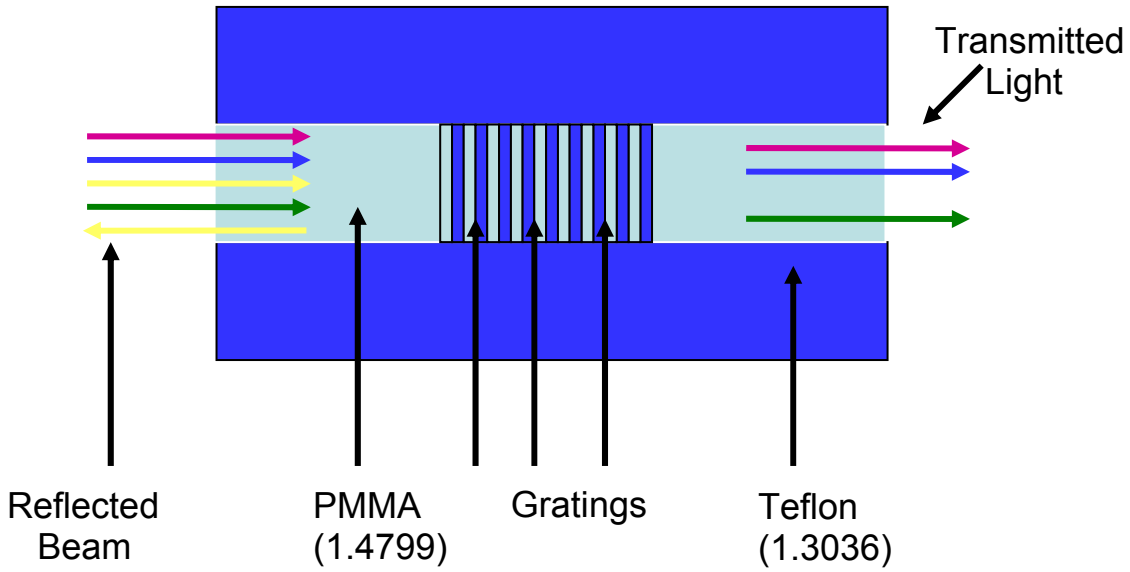

Figure 1.1 Schematic of a Bragg grating in a Teflon-PMMA polymer waveguide. The reflected wavelength is indicated by the yellow arrow.

The following figure illustrates the input and output spectra of a waveguide with an integrated Bragg grating.

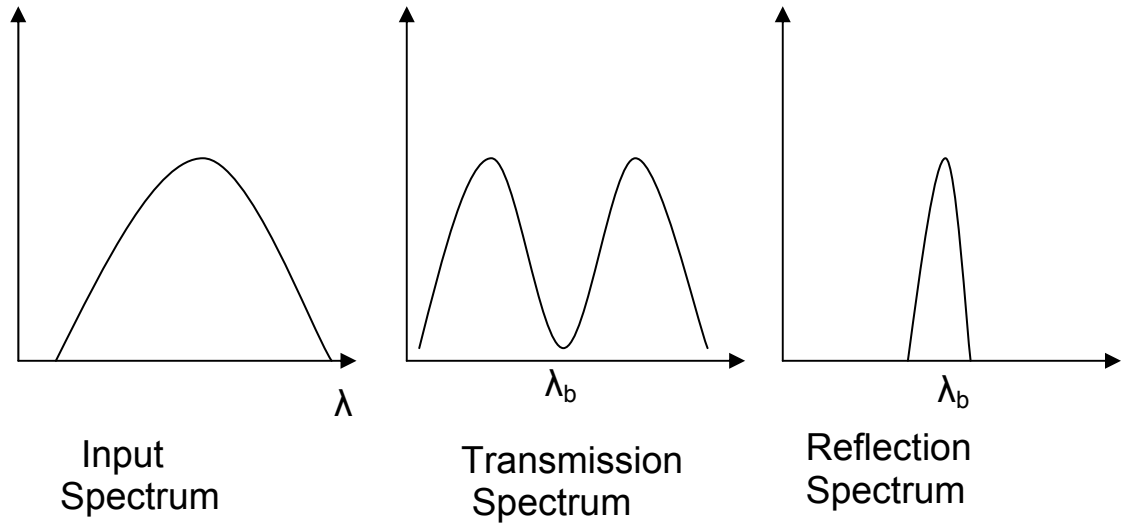

Figure 1.2 Input and Output Spectra of a waveguide with a Bragg grating.

In this thesis we have successfully demonstrated a novel fabrication method to make the polymer waveguides. PMMA forms the core and Teflon forms the cladding. A detailed description about the fabrication process is given in chapter three. The bulk of the project focuses on the fabrication.

1.4 Surface Plasmon Resonance (SPR)

Since last two decades there has been great research activities aimed towards development of optical sensors. Optical sensors play a key role in biological and chemical sensing. SPR is an optical phenomenon arising from the interaction of light with a metal surface. A surface plasmon wave is a charge density TM (transverse-magnetic) wave which propagates along the interface of a metal and dielectric. SPR occurs when a thin metal film with negative permittivity is surrounded by a material with positive permittivity. At optical wavelengths gold, silver and copper exhibit negative real permittivity. However gold is the most widely used metal for SPR based sensors because of its chemical stability and abundant surface fictionalization techniques [6].

Surface plasmon waves can be excited by light when the energy and momentum of the incident photon and the surface plasmon wave match. When this happens the energy of the photon is transferred to the charge density wave at the interface. For a given angle of incidence, coupling to the plasmon wave occurs at a specific wavelength and is visible as a dip in the reflection spectrum. Since an evanescent electric field extends away from the metal surface into the surround dielectric, changes in the optical properties of the dielectric will cause the resonance dip to occur at a different wavelength. This phenomenon forms the basis of sensing.

The resonance condition is not satisfied when the light is incident directly at the metal-dielectric interface. Momentum of the incident photons should be altered to achieve the resonance [7]. There are three often used configurations, prism couplers, optical waveguides and gratings, often used to couple surface-plasmon waves. We have used BK-7 glass prism coupler in this thesis.

1.5 Why Long Range Surface Plasmon (LRSP) and SiO2

To distinguish refractive index and surface binding simultaneously at the same location, using single beam one needs to have LRSP and SRSP occur at the same wavelength. We need two resonant dips to identify two changes simultaneously. This occurs when a metal is surrounded by dielectric material of similar refractive index. In 1990[8], Matsubara et al. presented an angle modulated sensor based on LRSP. For LRSP to occur, the metal layer and prism should be separated by dielectric whose refractive index is closely matched to that of the analyte. Since most of the analytes are in aqueous solution, with refractive index close to that of water, a dielectric with a refractive index similar to that of water would permit a LRSP. Thus Teflon AF-1600 (1.30368) is an ideal choice for LRSP to occur. Homola et al. have successfully demonstrated a wavelength modulated sensor based on LRSP. The reflection spectrum they measured is similar to that shown below. Thickness of Teflon AF-1600 and gold layers used in the simulations are the same as they used.

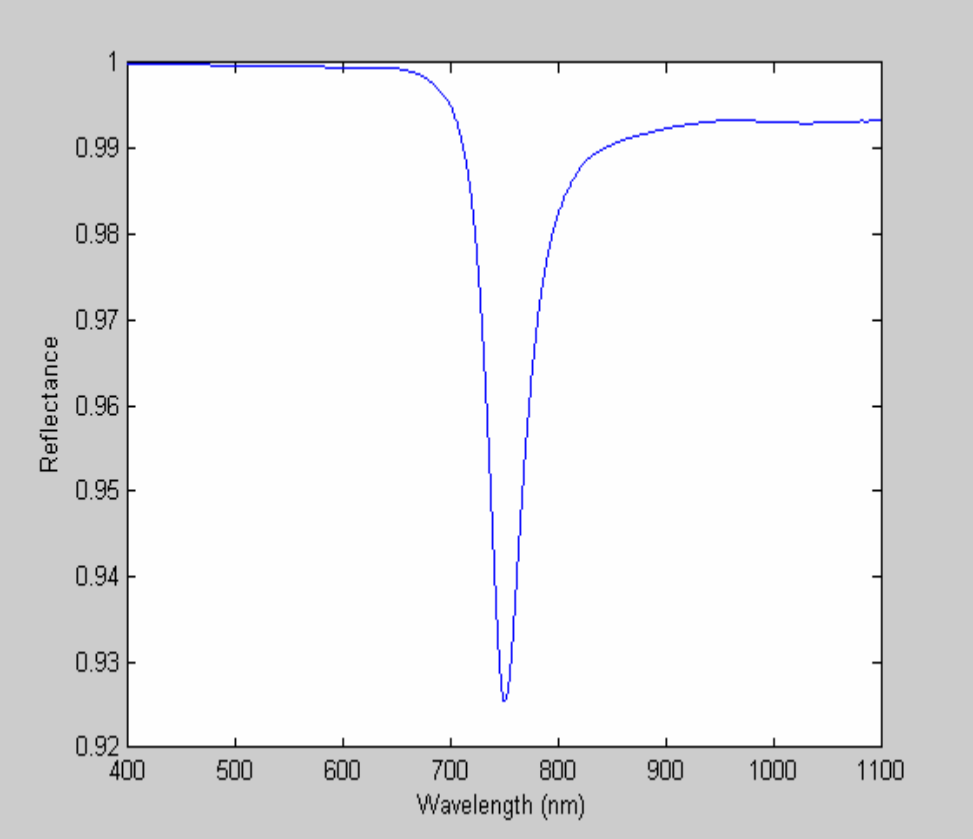

Plot 1.1 Simulated reflection spectrum obtained when coupling to a long-range surface plasmon wave supported by a Teflon-Au-Water structure. Good agreement was obtained with the experimental results of Homola et al.

However, Homola et al did not couple to both LRSP and SRSP wave simultaneously. For effective self referencing one should be able to get measure the response of both modes simultaneously for the same angle of incidence. With careful selection of the thickness of the metal layer this can be achieved, and light can be made to couple to both the long and the short range surface plasmons. Thus we see two different dips in the reflection spectrum. When this happens, one can observe two couplings – long range surface plasmon (LRSP) and short range surface plasmon (SRSP). SRSP is concentrated more near the metal surface and is more effective in sensing surface binding processes common in biochemical sensing. On the other hand both modes should be

similarly effective in sensing bulk refractive index changes. For self-referenced sensing, it is only important that the modes exhibit different sensitivities for solution refractive index changes and for surface binding.

The plot below shows both LRSP and SRSP occurring at the same angle of incidence.

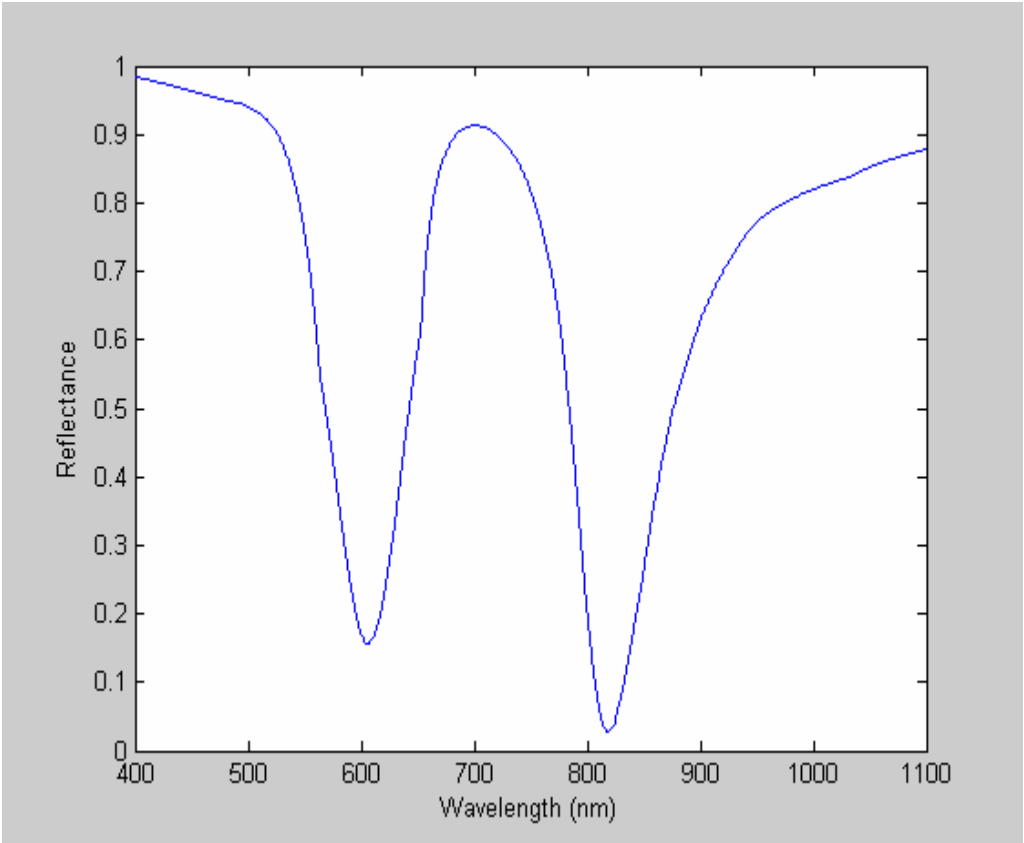

Plot 1.2 Simulation Plot with Teflon and Gold Layers where the Teflon and Gold thicknesses were 500nm and 55nm respectively and the angle of incidence was 68^0

In this thesis work, we have fabricated a self referencing SPR sensor using Teflon as one of the dielectric layer. Gold is evaporated on the Teflon to form the metal layer. Formation of (Octadecanethiol) ODT layer was used to demonstrate self referencing action of the sensor. Surface binding sensitivities and bulk refractive index sensitivities are measured using the following equations.

$$\Delta\lambda_{\mathrm{LR}} = S_{\mathrm{S\text{-}LR}}\,\Delta t + S_{\mathrm{B\text{-}LR}}\,\Delta n_B \tag{1}$$

$$\Delta\lambda_{\mathrm{SR}} = S_{\mathrm{S\text{-}SR}}\,\Delta t + S_{\mathrm{B\text{-}SR}}\,\Delta n_B \tag{2}$$

LR and *SR* denote long range and short range respectively, Δn_B and Δt are bulk refractive index change and thickness of the ODT layer respectively. Δn_B is obtained from the measurements of Albuquerque et al [9] and Δt can be known from the data of Whitesides et al [10]. The same device can be modified to sense non – specific binding in analyte when part of the gold layer is masked and SiO_2 is evaporated on the exposed gold surface. For practical purposes the gold surface will be functionalized to bind to a specific target and SiO_2 surface would remain non-functionalized. Thus the target body will bind only to gold and not to SiO_2; anything that binds to both the surfaces is not the target substance. Christina Boozer et al [11] fabricated a similar sensor using Tantalum pentoxide on gold surface; however, this sensor did not support both long- and short-range surface plasmons. As a result, the sensor relied on a spatially separate reference regions to measure background refractive index changes.

Later chapters explain more about the fabrication and modeling of these devices. Functionalizing of the sensor surface has been tested using ODT layer. ODT, when flown through the sensor binds only to the gold surface and not to SiO_2. When the optical input beam overlaps both the exposed gold and the SiO_2 coated regions one should observe three resonance dips on the reflection spectrum. However, this is only possible with precisely controlled material thickness and film quality. Unfortunately equipment problems prevented us from measuring film thicknesses for the fabricated sensors and hence the experimental results could not be correlated with our simulations.

However we could successfully demonstrate that the device with optimization can function to detect non-specific binding.

Chapter 2

MODELING

2.1 Overview

To begin fabricating devices one need to know their optimum dimensions. This chapter explains the theoretical modeling used to obtain the dimensions according to which devices were fabricated. Methods for modeling Bragg gratings in waveguides and SPR sensors are discussed here.

All results in this chapter were obtained numerically using Femlab and Matlab. Femlab is a multi-physics modeling tool which solves partial differential equations (PDE's) using the finite element method. Femlab has a special electomagnetics library, which was used for modeling horizontal (width) and vertical (thickness) dimensions. Femlab was used to solve the full vector wave equations for either the electric or magnetic fields.

$$\nabla^2 E + \omega^2 \mu \varepsilon E = 0$$

$$\nabla^2 H + \omega^2 \mu \varepsilon H = 0$$

2.2 Modeling a Channel Waveguide

All waveguides are modeled using perpendicular hybrid mode, in the electomagnetics module of Femlab. A channel waveguide is the simplest model discussed and therefore is a good place to start. Bragg-grating model will be built on the methods used for channel waveguide models. The waveguide is modeled in 2-D. First step is to draw a channel waveguide model using Femlab CAD tool. In the Femlab results

presented in this thesis, the X-axis represents the width in meters, of the materials and Y-axis represents the thickness (in meters). The following drawing shows a channel waveguide.

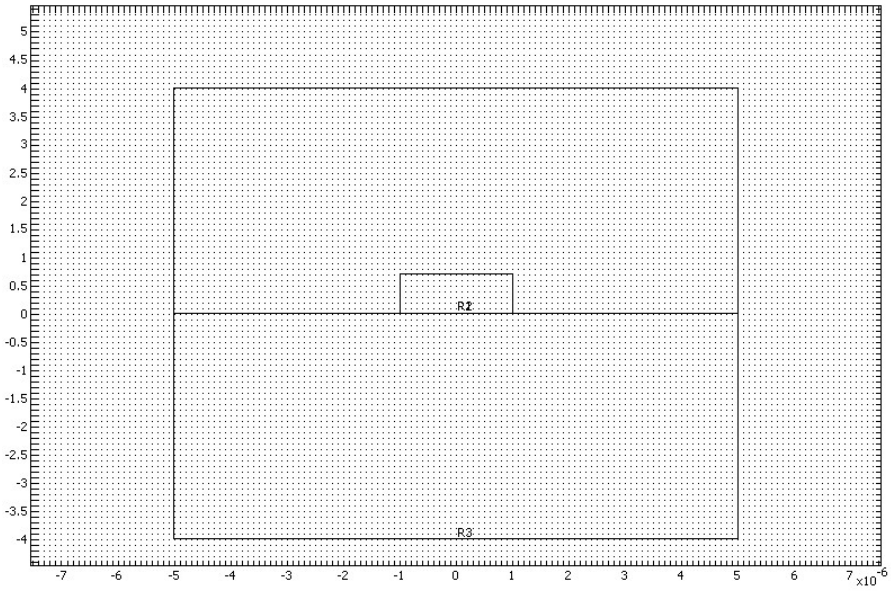

Figure 2.1 CAD Drawing of Channel Waveguide

Next refractive indices of Teflon and PMMA at 1550nm and boundary conditions are to be specified. The following specifications are used for the channel waveguide.

Teflon AF-1600 = 1.3036

PMMA = 1.4799

There are eight boundaries in the channel waveguide structure. All the Boundary conditions were set as perfect electric conductors.

$$n \times E = 0$$

The wavelength used is 1550nm as the waveguide were modeled for communication purpose. Once done with drawing the waveguide, we automatically generate the finite-element mesh. The mesh can be refined to get more accurate results.

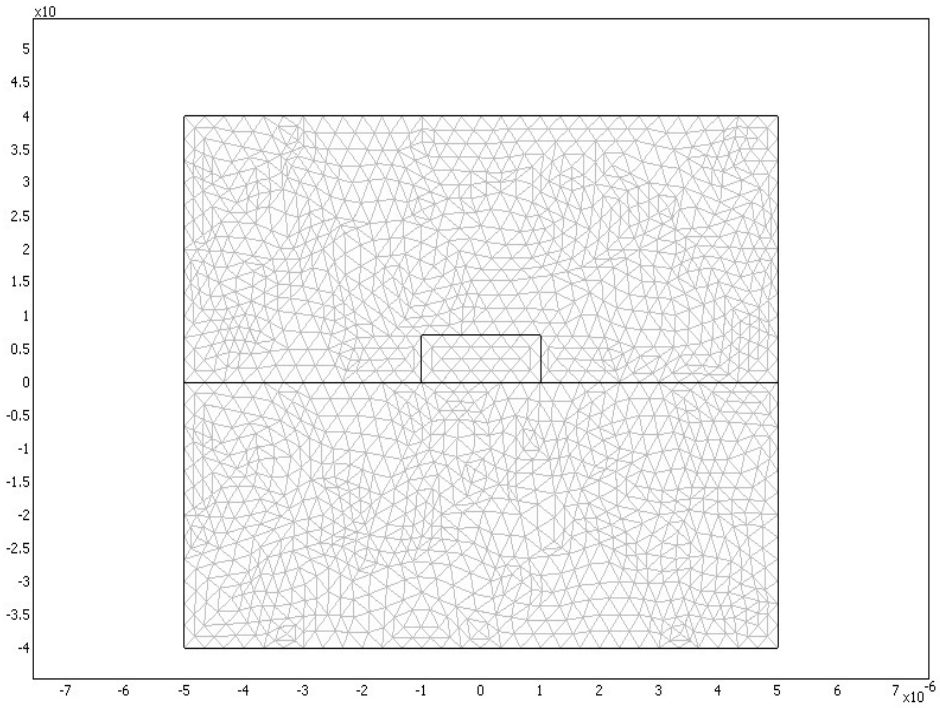

Figure 2.2 Channel waveguide with mesh used for analysis.

Finally the solver is invoked to solve the PDE's. The result obtained is shown in the following figure. The figure illustrates the modes in the waveguide for those particular dimensions.

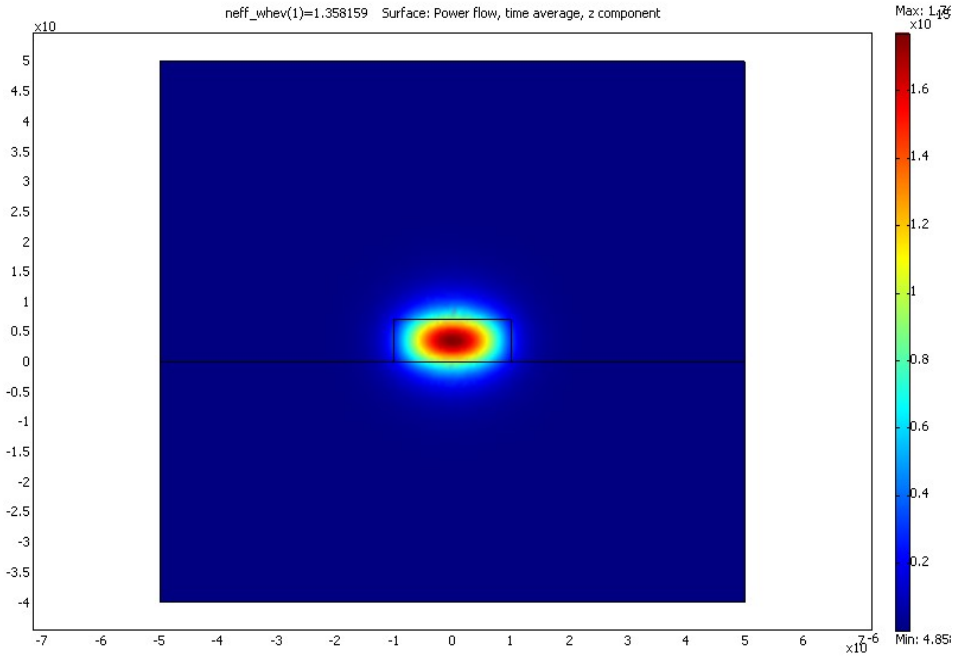

Figure 2.3 Solver result showing the modes in the waveguide for a particular geometry.

2.3 Modeling PMMA thickness

Since waveguides are designed for communication purpose, simulations were done to find the dimensions which result in single mode waveguides. Dimensions of PMMA are critical as it forms the core of the device. Initially arbitrary dimensions of Teflon were chosen as width = 10microns and thickness = 4microns. Keeping these fixed dimensions of PMMA in X and Y directions were varied. Simulations were performed with different dimensions of PMMA. Basing on the results, waveguide becomes multimode when thickness of PMMA exceeds ≈ 1micron and width exceeds ≈ 2microns.

Hence PMMA thickness was fixed at 0.7microns. This thickness was chosen because it is within the range of obtainable from spin coating PMMA. Moreover we get a margin of error of 0.3 microns. The following figure shows that waveguides tends to become multi mode when the width of PMMA is 2.5 microns and the thickness is 1.5 microns.

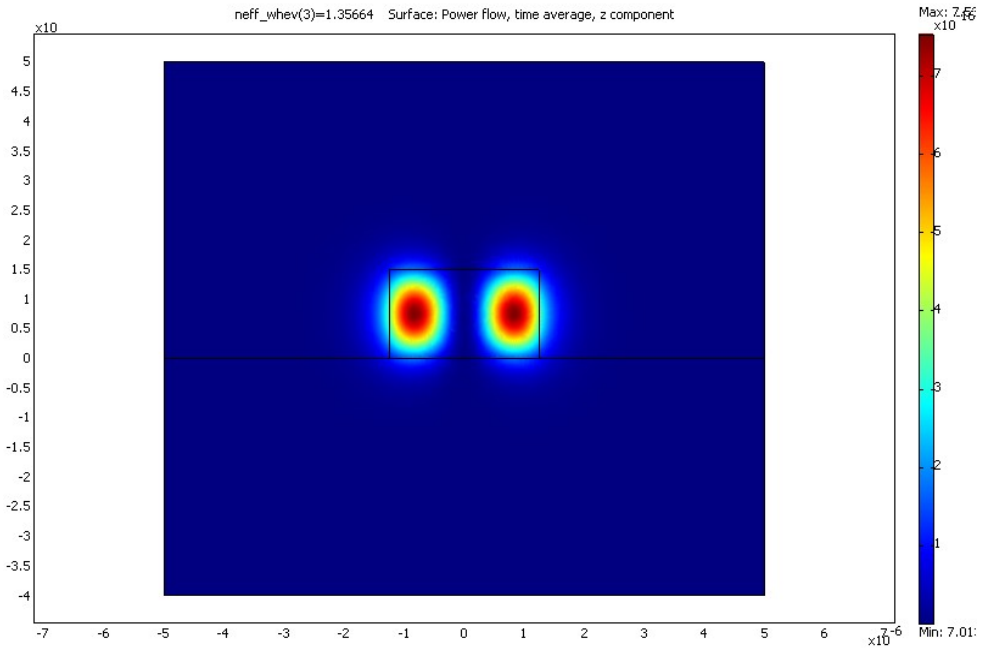

Figure 2.4 Higher order mode in a channel waveguide when PMMA thickness exceeds 1micron

2.4 Modeling Teflon thickness

Once the core dimensions are fixed, simulations were done to find the optimum lower cladding thickness for Teflon on a silicon substrate. In this case the waveguide mode is not of a concern. The key criterion was power loss. Dimensions were chosen to provide acceptable power loss. Because of the high index contrast any reasonable Teflon thickness essentially eliminated mode overlap with the substrate. As a result, power loss

to the substrate was not a serious concern. The Teflon thickness was fixed at 4 microns because we knew the spin speed to get 4 micron thickness.

The more important parameter was the separation of the PMMA core from any surrounding PMMA. Since PMMA is a positive electron beam resist, the core is left unexposed and the surrounding regions are exposed. We would like to minimize the area required for e-beam exposure, so we needed to find the lateral separation that provided acceptable power loss. The power in the waveguide mode was reduced by -35db when the core was 5 microns from any surrounding PMMA, and -50db when the core was 10microns or farther. Hence a width of 10 microns was chosen. It can be observed from the figure below that it is much less when the width was 10microns.

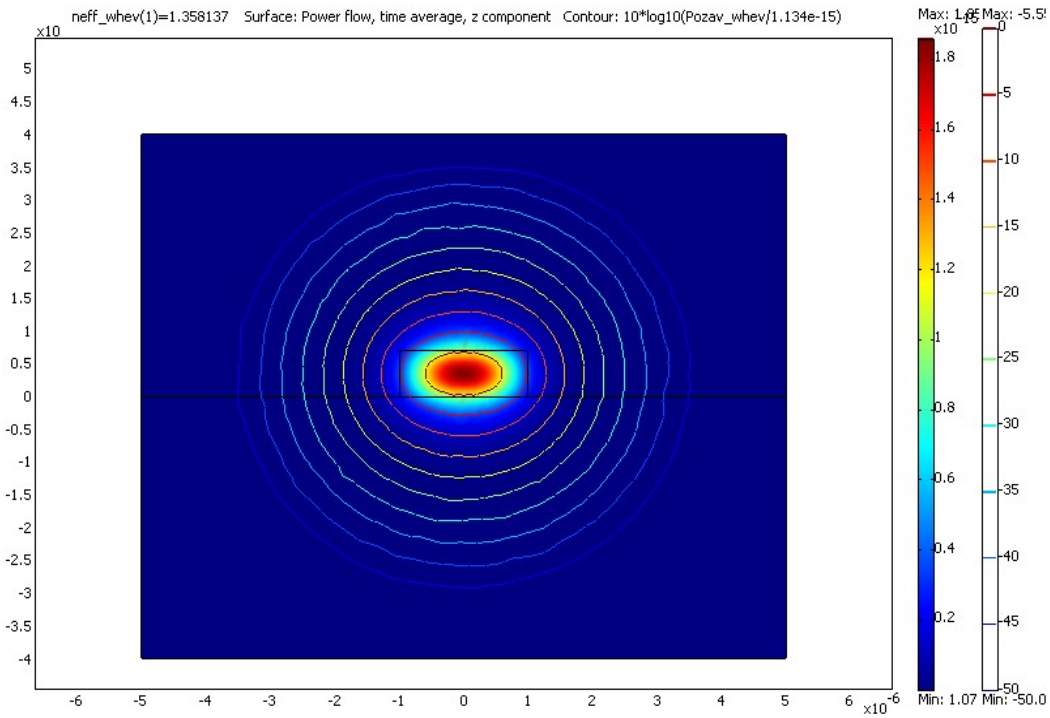

Figure 2.5 Contours of constant modal power (log scale) indicating the required separation of the PMMA core from any surrounding PMMA. The modal power is reduced by -50dB 10μm away from the core.

From the above figure it is clear that all the power is confined to the Teflon, when separation from any adjacent PMMA is 10microns. The final dimensions of the channel waveguide are as follows:

$width_p$ = 2 microns $width_t$ = 10 microns

$thickness_p$ = 0.7 microns $thickness_t$ = 4 microns

2.5 Design of Bragg Gratings in Polymer Waveguides

The Bragg grating model was setup up almost identical to the channel waveguide with the exception of the gratings in sidewalls of the core. All boundaries are still specified as perfect electrical conductors. All the properties of PMMA and Teflon are also the same. The refractive index for the gratings region was 1.39. Now that the dimensions of the core and cladding are fixed, the only the grating dimensions are to be changed. Here we were aiming for waveguides with grating strength between 60/cm and 100/cm.

The grating period for a wavelength of 1550nm is 565.7nm as obtained from the equation in section 1.2. The CAD drawing of a waveguide with grating is shown in the figure.

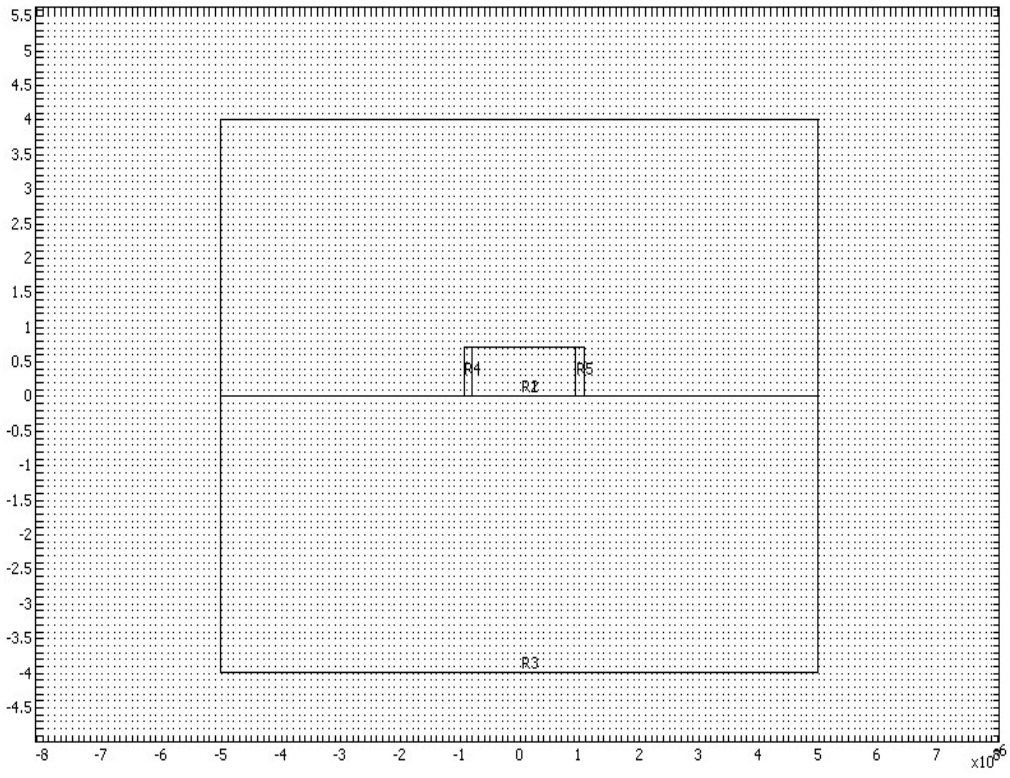

Figure 2.6 CAD Drawing of Gratings in a PMMA-Teflon channel waveguide.

2.6 Procedure to find grating strength

Grating strength for TE mode is given by [12]

$$\kappa = \frac{k_0^2}{2\beta\pi}(\eta_{core} - \eta_{cladding}) \frac{\iint_{gratings} E_x * conj(E_x)}{\iint_{waveguide} E_x * conj(E_x)}$$

(Replace E_X with E_y to find grating strength in TM mode)

where $\frac{k_0^2}{2\beta\pi} = \frac{1}{\lambda\eta_{eff}}$

η_{eff} is obtained for a given dimension, from simulating the waveguide in Femlab.

Ex and Ey denote electric filed in X and Y directions and λ = 1550nm.

The values for the integrals are obtained by performing sub domain integration in Femlab over gratings and waveguide. The below figure shows the GUI for performing integration (integration is performed over the selected region, integration value is shown at the bottom of the window)

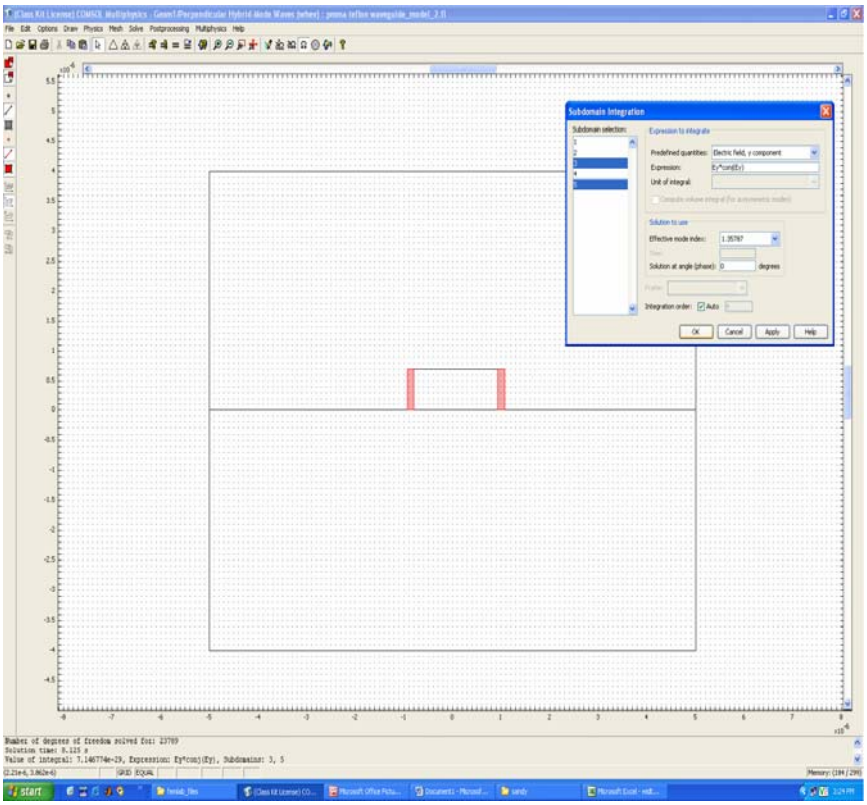

Figure 2.7 Integration over the grating region using Femlab.

Both effective index and grating strength change with depth of the grating teeth

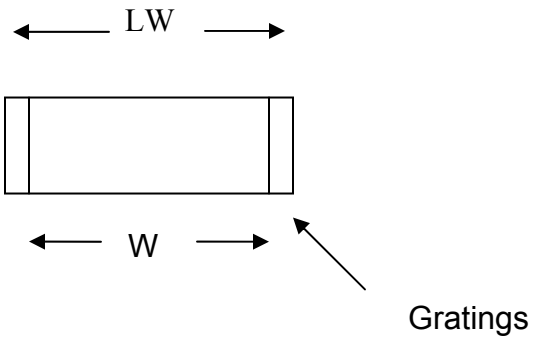

As the grating teeth come closer the width of the waveguide core, 'W' decreases and 'LW' increases. Their difference is the depth of the grating teeth. Grating strength was calculated for various grating dimensions, varying lengths of LW and L. The plot for grating strength, Grating Teeth Depth vs. Grating Strength is shown in the figure.

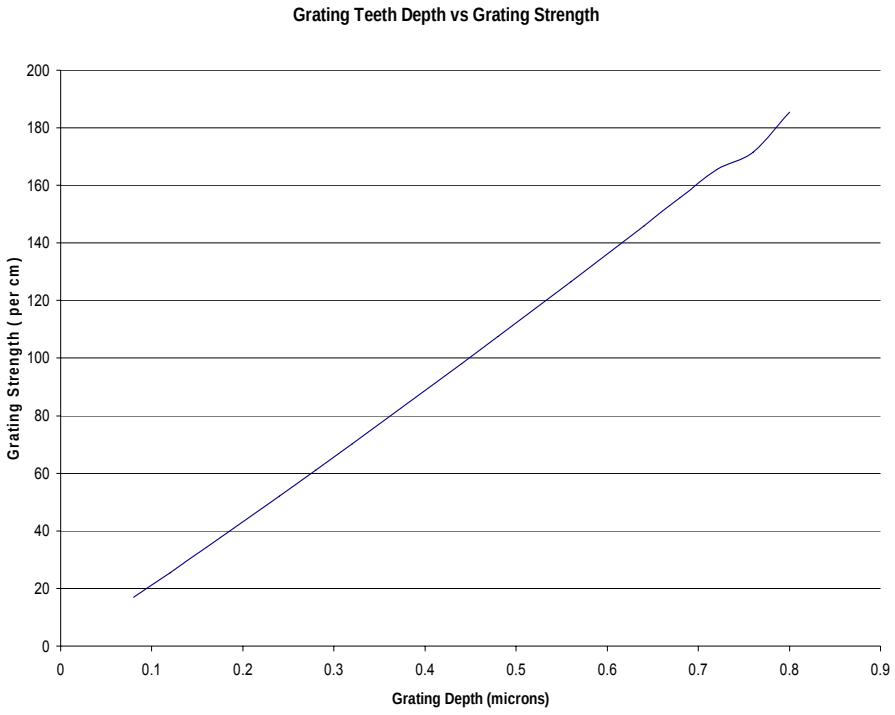

Plot 2.1 Grating Depth vs. Grating Strength

Waveguides with suitable grating strengths were patterned in the Raith50 Universal e-beam lithography tool.

Thus with all the waveguide dimensions fixed, waveguide patterns are drawn in the Raith software. They are such that average width of the core is 2microns.

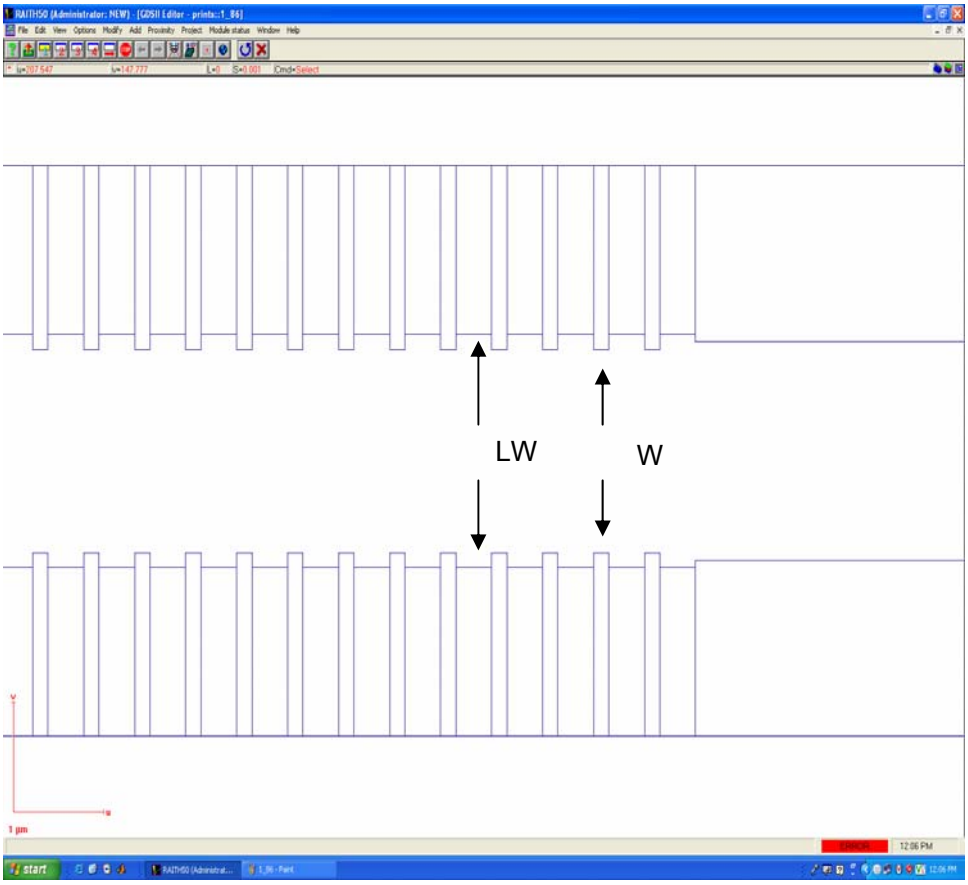

Figure 2.8 Gratings Pattern in Raith50

Dimensions of 'LW' and 'W' were chosen such that their average was always 2microns.

2.7 Modeling Self Referencing SPR Sensor

Modeling for the sensor was done using custom software written using Matlab. Only Teflon AF-1600, gold, SiO_2 thickness and angle of incidence were to be decided. We began with the thickness used by Homola et al. Refractive index of Teflon AF-1600 as a function of wavelength was calculated using the measurements of Lowry et al [13]. This data was used to determine the refractive index of Teflon AF-1600 in the infrared region from Cauchy's dispersion formula fit. Measurements of J.A.Woolam Co were used to find refractive index of gold as a function of wavelength.

The refractive index measurements were used to plot dispersion relations of LRSP and SRSP. Dispersion relations, plotted by simulating a thin gold film surrounded by Teflon AF 1600 intersect with that of BK-7 prism at two distinct wavelengths [6]. At these points the coupling to the surface plasmon modes will be strongest. Thus light couples to the LRSP at shorter wavelength and to SRSP at longer wavelength.

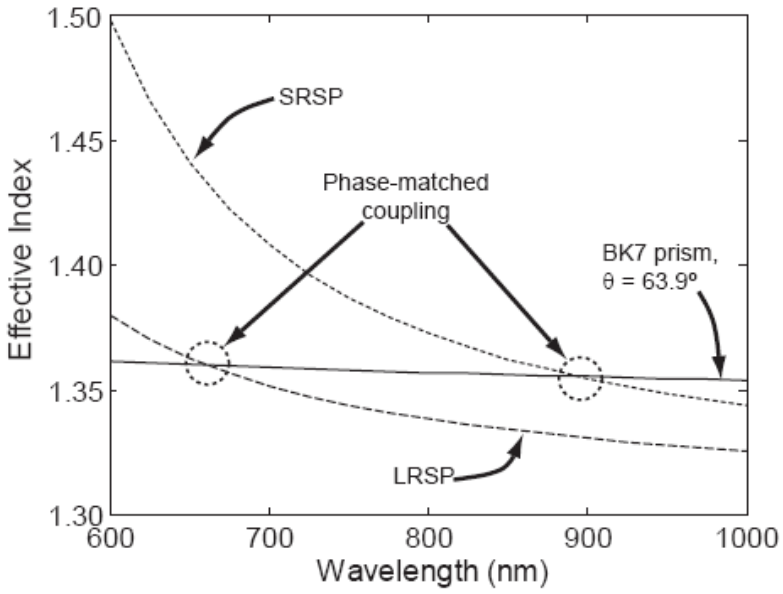

Plot 2.2 Dispersion Relations of SRSP, LRSP and BK-7 Prism

The Thickness of Teflon AF-1600, gold and SiO_2 play key role as they can alter the coupling and self referencing may not be obtained if they are different from the specified values. The final stack of materials for the SPR sensor is drawn below:

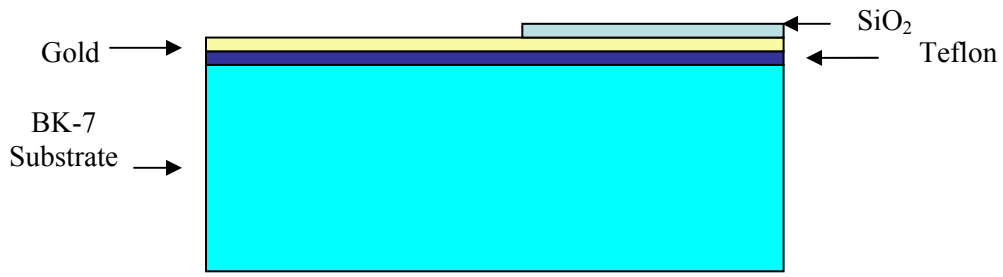

The Matlab simulations were performed to find the thickness of these materials.

One should get a reflectance spectrum as shown in the below plot for 500nm of Teflon AF-1600, 50nm of SiO_2 and 55nm of gold and the angle of incidence is equal to 68^0.

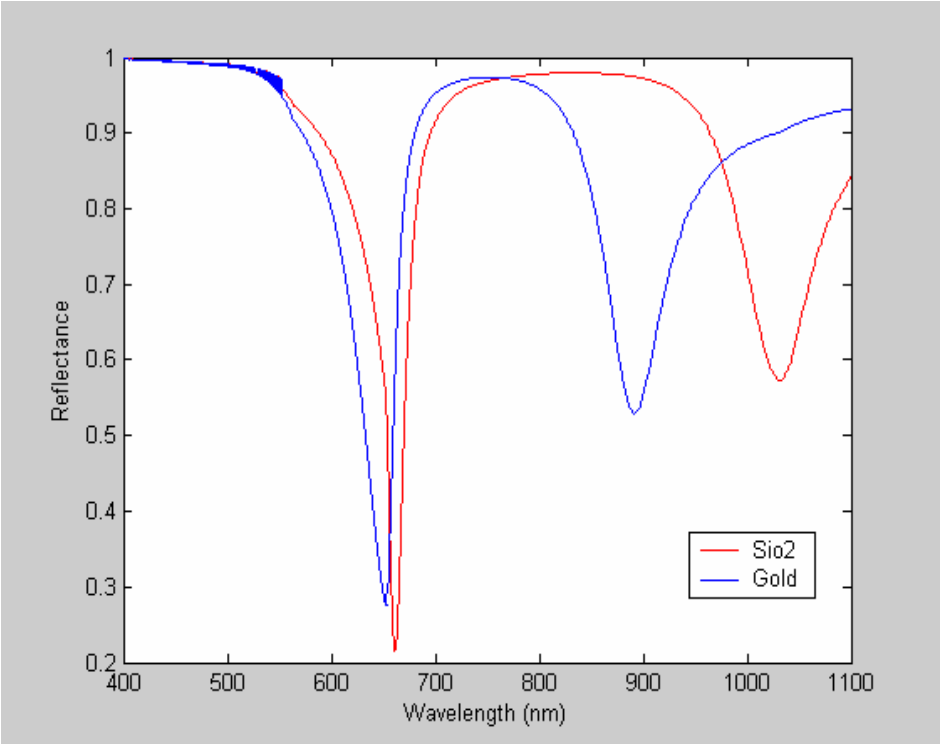

Plot 2.3 Simulation Result when Gold = 55nm, SiO_2 = 50nm

Thicknesses play a very crucial role in the functioning as sensor. We simulated the sensor with various thicknesses of Teflon AF-1600 and gold at various angles. Simulations were performed to find out the right thickness for SiO_2 which can result in considerable amount of difference in the spectrum with and without SiO_2 layer.

Chapter 3

FABRICATION

Once the dimensions are fixed, the waveguides and the sensor must be fabricated. This is the most challenging part of the project. Since we were using Teflon, which was developed such that nothing sticks to it, making PMMA adhere to it was the most crucial part of the project. This chapter describes the fabrication steps for the waveguides and later gives way to the fabrication of SPR sensor. Due to the breakdown of the e-beam lithography (EBL) system, we couldn't go ahead with the e-beam exposure. But a detailed account of the steps for the exposure has been mentioned in this chapter.

3.1 Overview

First step is to clean the silicon wafer. Since the adhesion of Teflon to silicon is poor, adhesion promoter is first spin coated on the wafer. Next, Teflon is spin coated and soft baked to form the lower cladding. Later PMMA is spin coated on top of the Teflon and soft baked to form the core. After e-beam exposure and development, Teflon is again spin coated to form the upper cladding. But due to equipment trouble we later switched to fabrication of SPR sensor. The fabrication for the sensor is comparatively less complicated. For the SPR sensor, BK-7 glass substrate was used. Teflon was spin coated and gold was deposited on it. Later, half of it was masked and SiO_2 was deposited. Detailed explanation of the above fabrication process is given in the following sections of the chapter.

3.2 Fabrication of Bragg Gratings in Polymer Waveguides

The first step is to clean the silicon wafer. Since the wafer acts only as a smooth, flat substrate, it has negligible effect on the waveguide functioning. Hence rigorous cleaning procedures like RCA 1 and RCA 2 were not performed. The wafer is first sonicated in acetone to remove organic contaminations. Later it is rinsed with isopropyl alcohol (IPA) as cleaning with deionised (DI) water doesn't completely remove the traces of acetone. Then the wafer is blown dry with nitrogen. The wafer is then placed on a chuck, where it is held by a vacuum. The desired chemical is then dispensed using a simple dropper. The speed of the spin coater can be selected as required. Also the spin coater can be set to spin at a certain speed for the initial few seconds and then ramp up to a higher speed. The spin coater has two sets of speed controls and timers to accomplish this.

The thickness of the material after spin coating depends on the spin speed and the viscosity. All the materials are dissolved in a solvent; their concentration in the solvent sets the viscosity.

Since the Teflon doesn't adhere well to the Si wafer, prior to spin coating Teflon, adhesion promoter must be spin coated. The adhesion promoter used is 1H, 1H, 2H, 2H perfluorodecyltriethoxy silane (Lancaster Synthesis, Inc.). Adhesion promoter solution is made by mixing 2% of adhesion promoter with 95% ethyl alcohol and 2% water. It is spin coated at an initial speed of 500 RPM for 12 seconds and then 1000 RPM for 30 seconds. First speed spreads the solution on the sample and second evaporates the solvent. The speed and time in this case are not of much importance as the adhesion promotion layer is essentially one molecule thick and doesn't interfere with the device

performance. The device is then soft baked at 110^0C for 10 minutes to evaporate any residual solvent.

Now Teflon is spin coated on the adhesion promoter layer. The Teflon used for our devices is Teflon-AF 1600(Dupont, Inc.). There are different solvents for Teflon-AF 1600 and the finding the right solvent is very important as the entire fabrication depends on this. More on this will be discussed in section 3.3 of the chapter. Teflon is spin coated at 500 RPM for 12 seconds and then at 1000 RPM for 30 seconds. The sample is then soft baked at 180^0C for 15 minutes to let all the solvent evaporate. This combination of spin speed gives a thickness of 4 microns.

Next step is to spin coat PMMA (polymethyl methacrylate), provided by MicroChem, on Teflon-AF 1600. This was one of the major hurdles and took several months to figure out a way to make PMMA stick to Teflon-AF 1600. Since nothing sticks to Teflon-AF 1600, PMMA would fly off the wafer as soon as the spin coater was started. After much thinking and research, it was found that oxygen plasma etching solves the problem of adhesion. This was a kind of break through in the project as it opened several directions to proceed

The Teflon coated sample is plasma etched at 50% power for 60sec in a custom made Plasma-Preen system. It is manufactured from a microprocessor controlled microwave and uses the relevant digital control functions present on the microwave. It also has an analog power control feature to provide a wider control over the plasma power. The system operates by the flow of a process gas (we used oxygen) at reduced pressure (~ 2-5 Torr) through the process chamber (inside which sample is placed) and

exciting the plasma discharge. The process produces ionized gas particles which react with the sample surface.

Figure 3.1 Plasma Preen Etch System

Figure 3.2 Plasma Etch Chamber

The mechanism for improved adhesion is still an open question. Some have hypothesized that the oxygen plasma etch roughens the Teflon-AF 1600 surface and creates grooves on the surface where PMMA would settle into during spin coating. However, the RMS roughness of the Teflon-AF 1600 coated surface was on average $10A^0$ greater than what it was before etching. The roughness was measured from Dektak 6M profiler (Veeco, Inc). This amount of roughness was not a concern as the Teflon-AF 1600 layer formed the cladding for the waveguide device. Therefore, we believe that oxygen atoms may replace some fluorine atoms in the Teflon polymer during etching. Normally, this reaction would be energetically unfavorable, but the presence of high energy ions may enable it.

Once plasma etched, PMMA is spin coated on the sample. For the waveguide device we used 4% PMMA in a cholorobenzene solution. A spin speed of 1000RPM for 30 seconds yields 0.7 micron thickness. This is confirmed from readings obtained from the Dektak 6M profiler. The spin speed curve provided by MicroChem also confirms the same. Here an important observation was made that if the sample is spin coated at a lower initial speed as done in case of adhesion promoter and Teflon-AF 1600, the later higher speed will have no effect on the PMMA thickness. The thickness of PMMA was observed to be around one micron if it was spin coated at an initial speed of 500 RPM and then at 1000 RPM. Hence the initial spinning should be eliminated. This is not surprising given that chlorobenzene is a highly volatile solvent and is likely to evaporate during the low-speed spin step. After spin coating PMMA, it is soft baked at 110^0C for 5 minutes to get rid of the residual solvent. The following block diagram describes the entire fabrication process.

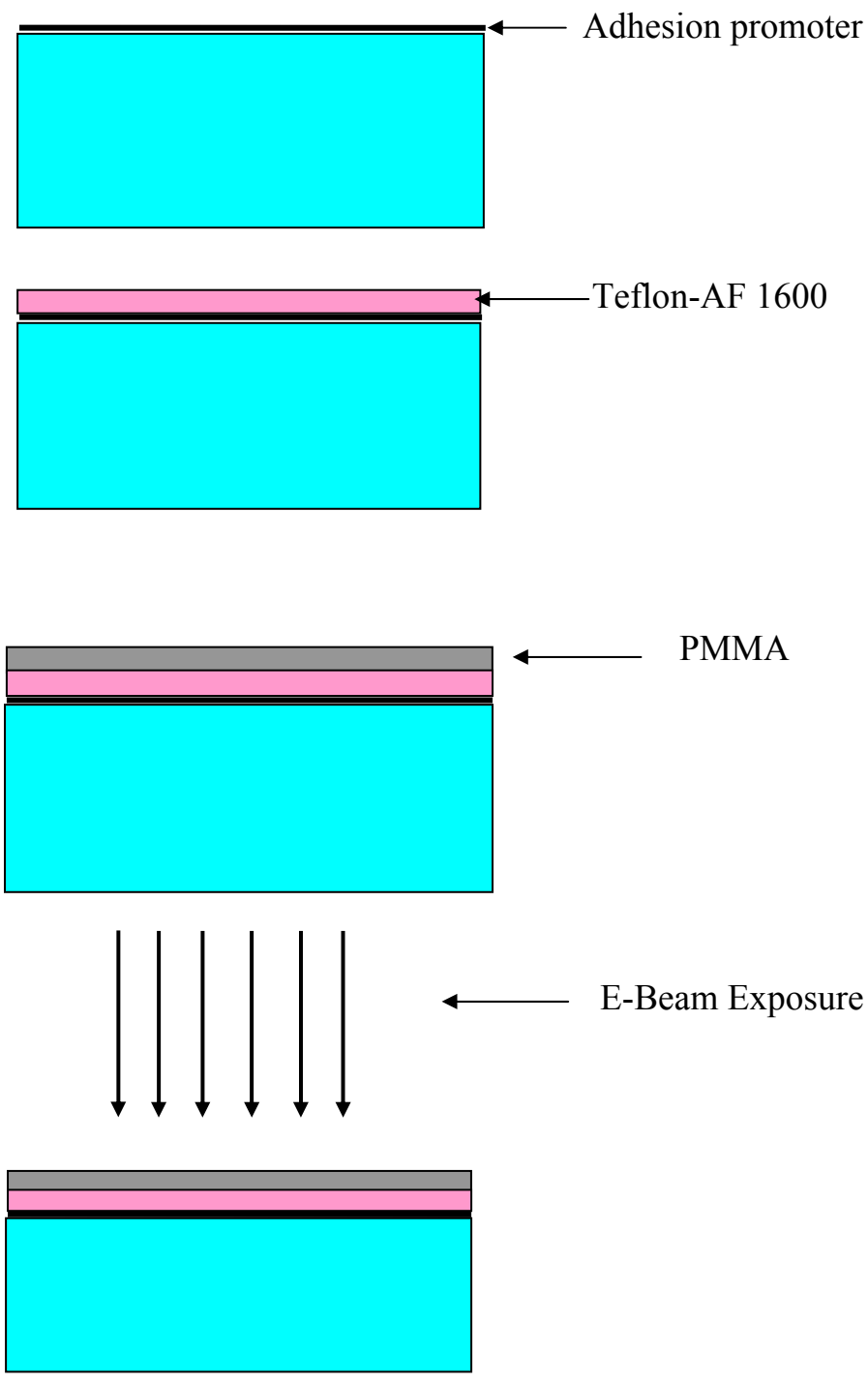
Adhesion promoter
Teflon-AF 1600
PMMA
E-Beam Exposure

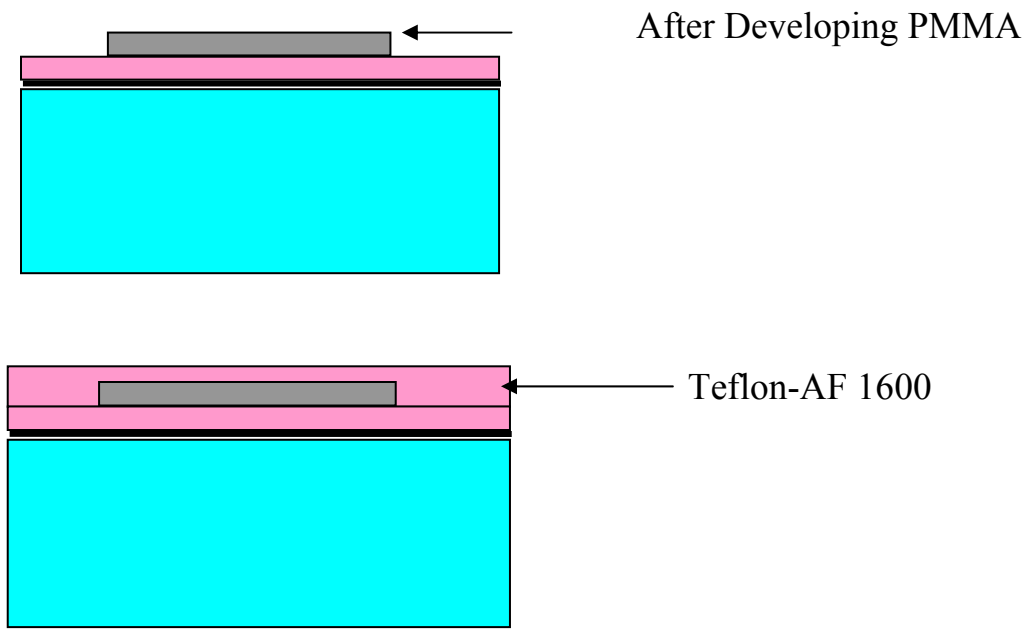

Figure 3.3 Fabrication Steps for PMMA-Teflon waveguides

Now the sample is ready to write a waveguide pattern on it. Next task is to draw a waveguide with gratings pattern. The sample will then be loaded into the e-beam lithography system and the drawn regions will be exposed to electron beam. In e-beam lithography, electrons, instead of photons, which are used in the photolithography system, are used to write patterns. E-beam lithography system consists of electron source, vacuum chamber and a stage to move substrate around. Electron stream is made to pass through electromagnetic lenses and focused into a small spot. E-beam lithography is much slower than photolithography; however, the system is not limited by diffraction and thus provides much higher resolution. The PMMA coated substrate is exposed to these electrons and the exposed area is developed away in 1:3 methyl-iso butyl ketone: IPA developer to obtain the required pattern

The pattern is drawn using Raith50 Universal E-Beam lithography tool. A Matlab code is used to generate a text file with desired coordinate positions for the gratings. This

text file is then loaded into the Raith50 tool to generate patterns. Patterns are drawn such that the average width of the waveguide is two microns as mentioned in the modeling chapter. The overlapping regions will be cancelled out so that they are not exposed twice. By changing the depth of the grating teeth one can obtain patterns with different grating strengths. The following figure shows the gratings pattern obtained from the tool

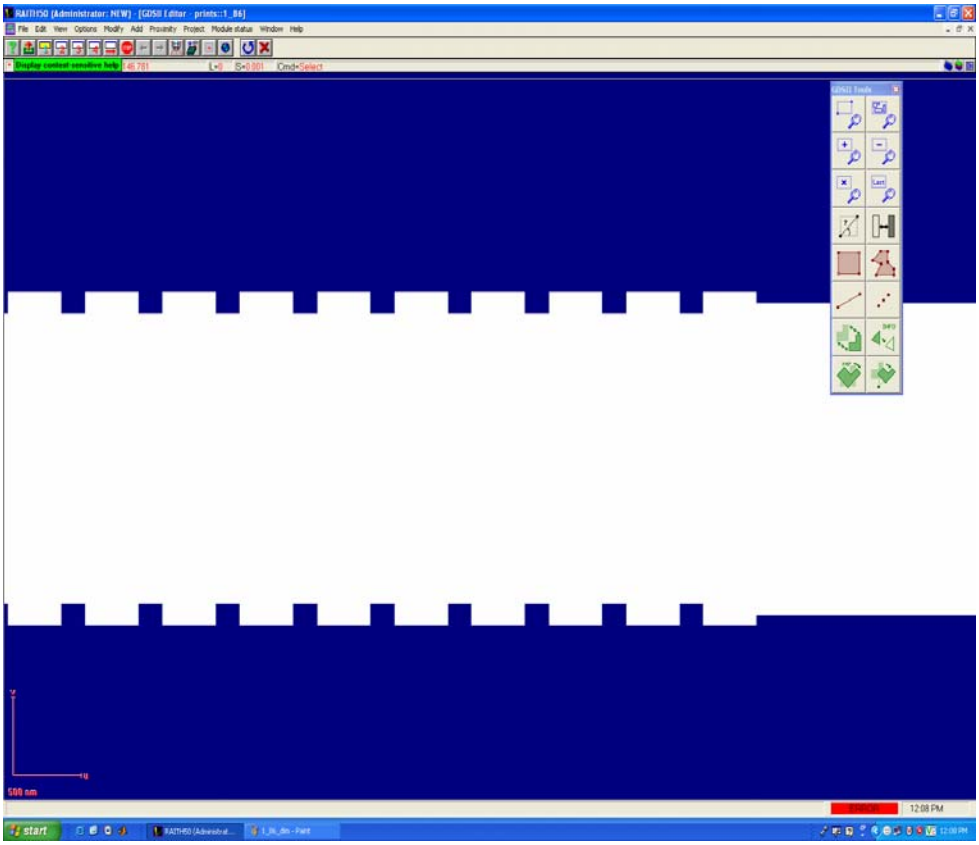

Figure 3.4 Grating Pattern Drawn in Raith50 Tool

The pattern is duplicated and the exposure dose was varied from 0.7 to 1.2 so that we can determine which provides best defined pattern. .

Now the sample and the pattern are ready to be exposed in the e-beam lithography system. The following exposure settings were proposed to be use in the system.

E beam Lithography Exposure Parameters

Table 3.1 Specifications Used in EBL to Write the Waveguide Pattern

Settings:	**Area:**
Beam Current = 0.4459 nA	Step Size = 0.0504
Write Field = 100 μm	Dwell Time = 0.011393
Magnification = 813X	Dose = 200
Line:	**Dot:**
Step Size = 0.0198	Dwell Time = 0.051073
Dwell Time = 0.012000	Dose = 0.022773
Dose = 2702.42	

Now the exposed pattern is developed in methyl-isobutyl ketone (MIBK): IPA in the ratio of 1:3 for 30 seconds and rinsed with IPA and DI water. This removes the exposed PMMA and what is left forms the core of the waveguide. Then again Teflon is spin coated on the waveguide and soft baked.

3.3 Problems with Teflon

There are different kinds of Teflon available from Dupont with different solvents, concentrations, and glass transition temperatures. We began our experiments using 6% (by weight) Teflon-AF 1600 in 3M's Fluorinert FC75 solvent. Concentration of Teflon-AF 1600 is not a problem as it can be reduced by diluting or increased by heating it to evaporate the solvent. However the kind of solvent used is more important as the roughness of the Teflon-AF 1600 layer depends strongly on the solvent. By not using the

right kind of solvent, the surface of the Teflon-AF 1600 coated sample can be very rough. The following figures show the surface of the Teflon-AF 1600 coated sample when FC75 solvent was used. These were taken from the Dektak6M profiler.

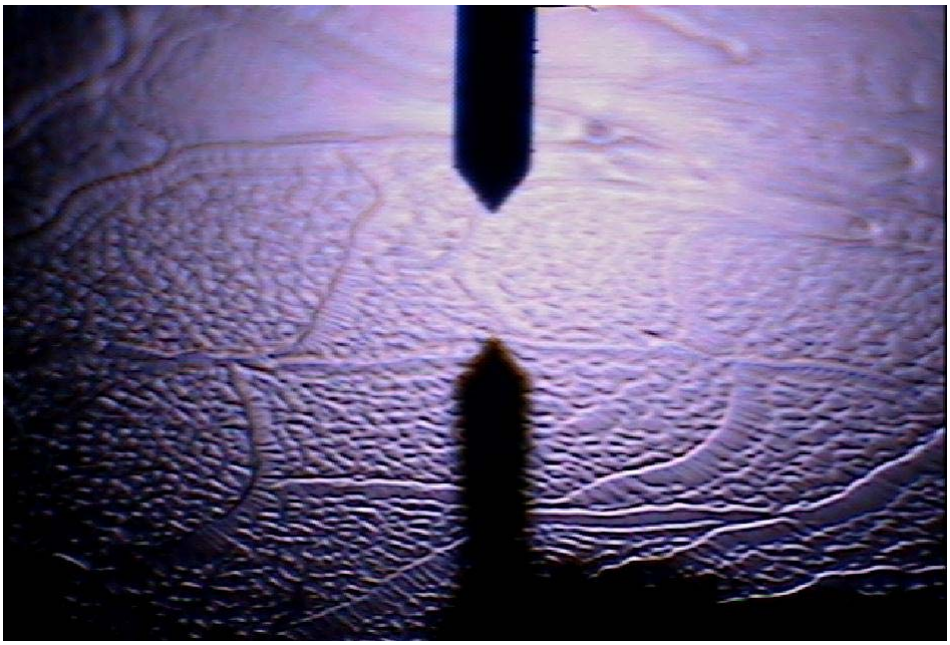

Figure 3.5 Rough Teflon Coated AF-1600, when Solvent is FC75

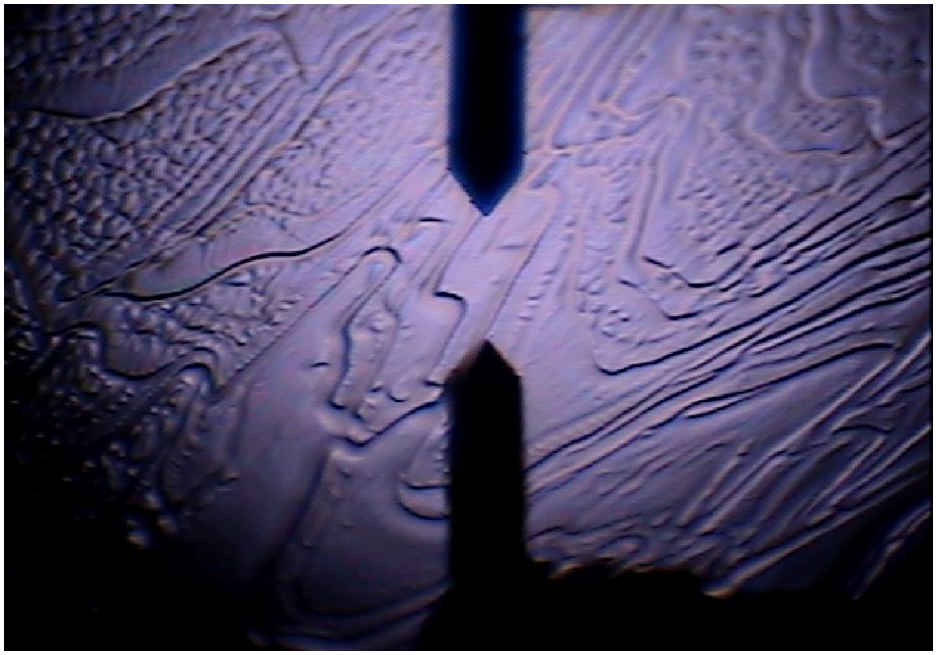

Figure 3.6 Rough Teflon AF-1600 Coated Surface

The roughness was measured to be greater than 500nm. This amount of roughness was not suitable for the either the waveguide or for the sensor design. Other groups have observed that higher boiling point (and thus less volatile) solvents yield lower roughness in spin coating. As a test experiment we exchanged the solvent used for coating Teflon-AF. The Teflon solution was heated at 60^0-70^0C to evaporate most of the Fluorinert FC-75 in it. Then we mixed the highly concentrated Teflon solution with Fluorinert FC-40(3M) which is a higher boiling point solvent. Now the solvent in Teflon-AF 1600 was largely Fluorinert FC-40(3M). This gave us a highly uniform and smooth Teflon layer as can be seen from the below figure.

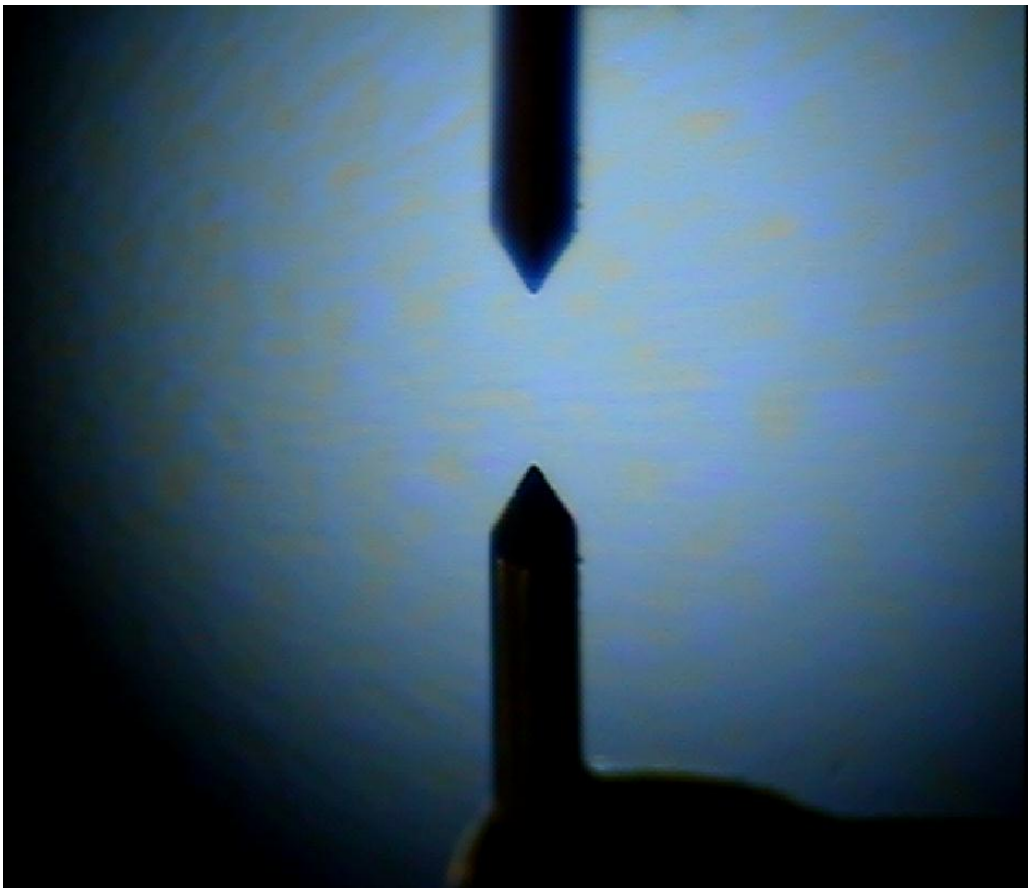

Figure 3.7 Smooth Teflon AF-1600 Coated Surface with FC40

The roughness reduced by 10 times, was found to be around 50nm. This was the first hurdle in the fabrication and it took a while to figure out the problem. Hence we later switched to a different grade of Teflon-AF 1600 which was provided at 18% by weight in Fluorinert FC-40. Since it was more concentrated, we diluted it with more Fluorinert FC-40 to reduce the concentration.

3.4 Fabrication of SPR sensor

The first step in any kind of fabrication is to clean the substrate. The substrate used in this case was BK-7 glass substrate (Esco Products, Inc). This one was chosen in particular because it matched the refractive index of the prism, which is the main component in the measurement setup, as will be discussed in the next chapter. The substrate comes in nicely polished square shape. It is sonicated in acetone and rinsed with IPA. Then it is blown dry in nitrogen.

Then adhesion promoter is spin coated using the same spin speed and baking temperatures as was used in the fabrication of waveguides. However there are few changes in the Teflon-AF 1600 spin speed as we required a much thinner film for the sensor. The Teflon-AF 1600 solution was further diluted with FC-40 to reduce the concentration to 9%. Also it was spin coated at a higher speed to get a thinner film. The spin speed used was 500 RPM for 12 seconds followed by 3000 RPM for 30 seconds. Then the substrate was soft baked at 180^0C for 15 minutes.

3.5 Deposition of Gold

Next a thin film of gold (99.9% gold pellets from Kurt Lesker, Inc.); of thickness 55nm was deposited on the Teflon surface. The gold was deposited using electron beam (e-beam) evaporation. The sample is placed inside the e-beam evaporator and the evaporator chamber is evacuated. A vacuum of 2.0x10-6 Torr was used for this experiment. An accelerating grid is raised to a voltage of 9 kV with respect to a filament. A current is then applied through the filament to heat it up. Electrons will then be released by phenomenon of thermionic emission. The filament current adjustment controls the electron beam intensity. The electron beam is then bent by a magnetic field and focused on a crucible filled with gold pellets. The focusing of the beam is accomplished by horizontal and vertical controls that vary the magnetic field. The gold starts melting when the filament current is high enough. Due to the high vacuum in the chamber, gold atoms evaporate from the crucible and will deposit on the sample substrate.

Figure 3.8 Electron-beam Evaporator

Though the same task can be performed using thermal evaporator, there is a possibility of getting a non uniform thickness of the film as the source size in that case would be large. Also e-beam evaporator offers more precise control on the film thickness.

3.6 Deposition of SiO_2

After gold deposition, the sample was taken out and an aluminum foil was used to mask half of the gold coated substrate. Silicon dioxide granules (Kurt Lesker, Inc) were evaporated in the e-beam evaporator. The same vacuum and voltage was used. After performing rigorous simulations on Matlab, we decided to go for a thickness of 50nm of SiO_2. Since the aluminum foil masked part of the substrate, SiO_2 was deposited only on

one half of the sensor. The structure of the SPR sensor after SiO_2 deposition would be as shown in the following diagram.

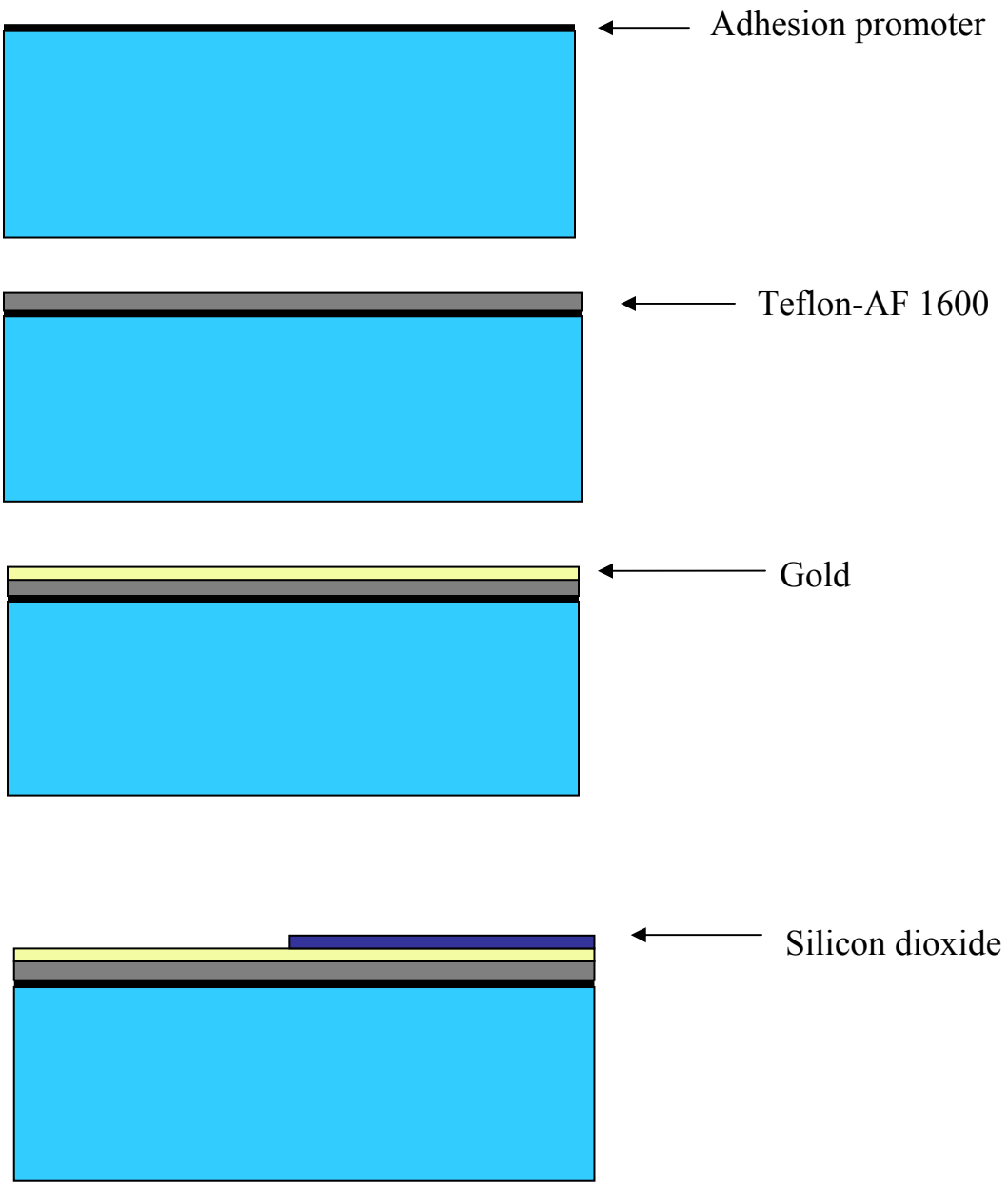

Figure 3.9 Fabrication Steps for Self Referencing SPR Sensor

Chapter 4

TEST SETUP and RESULTS

4.1 Measurements

Unfortunately we couldn't fabricate the Bragg gratings in waveguides due to the failure of the EBL system. Hence no experiments were done on it to verify its functioning. This chapter describes the test set up for testing the sensor and the results obtained from the experiments.

The overall goal of the test setup is to introduce incident light from a halogen lamp onto the SPR sensor and then collect the reflected spectrum and plot the resonance wavelength vs. time. The light must first be polarized as TE and TM and either of the two is selected for a particular purpose. The polarized light is incident upon the sensor. The schematic of overall setup can be seen in figure below [6].

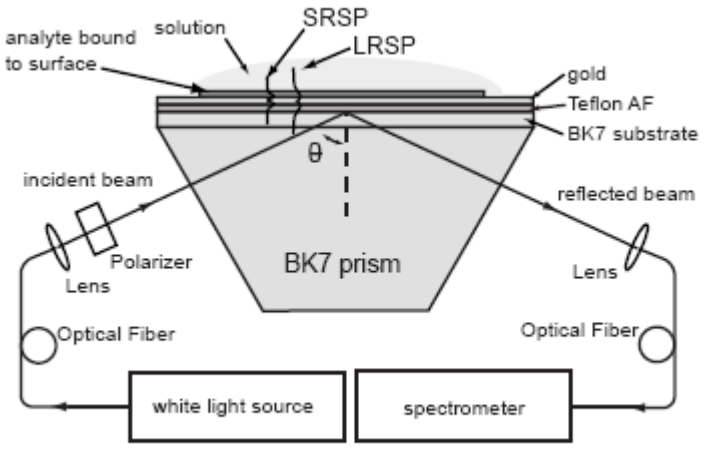

Figure 4.1 Schematic of Test Setup

The sensor, fabricated on BK-7 glass substrate, is mounted on BK-7 equilateral prism (Esco Products, Inc.). BK-7 specific index matching fluid (Cargille, Inc.) is used to bind the two so that there is no air gap. An ultra high molecular weight polyethylene (UHMW) flow cell is made to suit the dimensions of the prism and the substrate. The figure shows the flow cell and the prism arrangement. It is based on the Kretschmann prism apparatus.

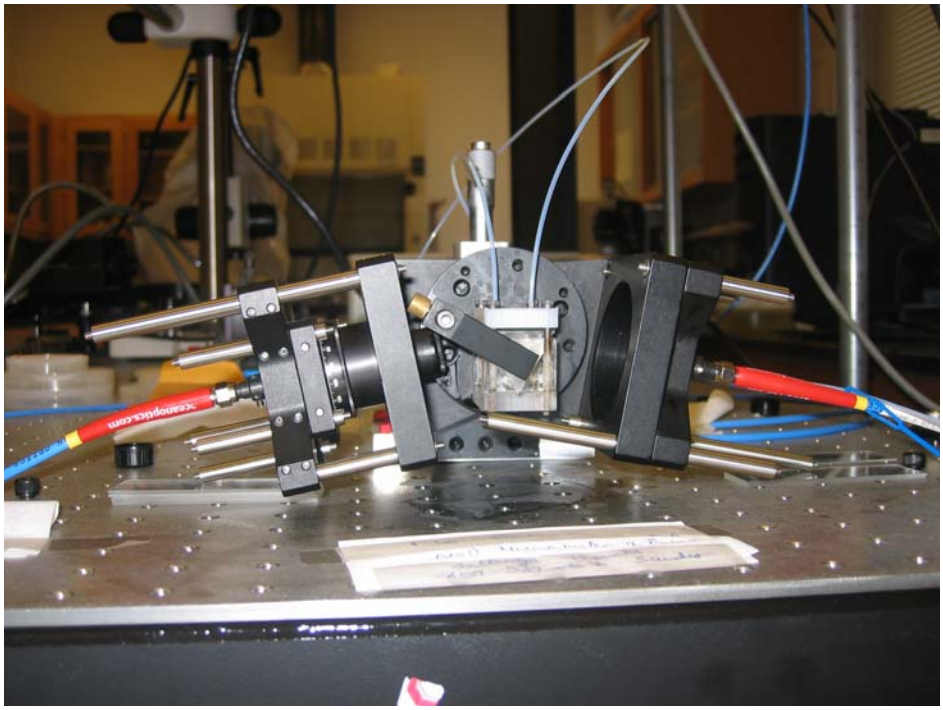

Figure 4.2 Sensor clamped with Flow Cell on Prism

It is sealed with a neoprene gasket. Liquids were flowed across the sensor surface through PTFE tubing. A vacuum pump and a liquid trap enable the flow through the tube. The flow trap consists of a 500 ml side arm Erlenmeyer flask maintained at 17 kPa and a polyetheretherketone (PEEK) micro metering valve (Upchurch Scientific) which controls

the liquid flow rate. The prism and the flow cell/sensor setup are mounted on a custom made, variable angle optical reference measuring system.

Light from a halogen lamp (Model DH-2000, Ocean Optics, Inc.) is sent into the measuring apparatus through a 200 micron core multimode optical fiber. A Glan-Taylor Polarizer (ThorLabs, Inc.), mounted on a rotation stage, can be adjusted such that either TE or TM wave is incident on the prism. A collimating lens focuses light from the fiber through polarizer and into prism and finally onto the sensor. A similar set up of lenses and fiber on the other side of the prism collects the reflected light. Here the fiber is routed to a computer controlled spectrometer (Ocean Optics Model HR-4000). A program is developed in Labview (National Instruments) to plot the data collected from the spectrometer. It plots the points of resonance vs. time.

4.2 Detection

To demonstrate the sensors self referencing capability, formation of ODT monolayer on the gold and SiO_2 is studied. ODT was dissolved in ethanol to form 3.2mM solution. Solutions of 2% and 4% by weight methanol in ethanol were also prepared. The solutions were introduced on the sensor in the following order:

(1) Ethanol (2) 2% methanol in ethanol (3) 4% methanol in ethanol (4) ethanol (5) 3.2mM ODT in ethanol (6) 4% methanol in ethanol (7) 2% methanol in ethanol. All experiments were done at room temperature using the flow rate of 0.0149ml/sec.

The following settings for the Ocean Optics spectrometer were used, while acquiring data: Integration time = 10ms, 10 averages per wavelength, Boxcar averaging of 50 wavelengths.

Prior to collecting data a dark spectrum was stored with the lamp turned off and was subsequently subtracted from all measurements. A reference reflection spectrum was taken using the incident TE wave. The angle of incidence was adjusted to place the LRSP and SRSP minima within the region of the spectrum with lowest noise. The measurement system can be adjusted such that the TM wave is incident either on gold or on SiO_2 region. The same experimental procedure is repeated when the TM wave is entirely incident on the SiO_2 region.

4.3 Experimental and Simulated Results

With careful selection of material thicknesses, light incident on the overlap of gold and SiO_2 should give three dips in the spectrum as shown in the plot. This is when the thickness of the gold is 55nm and that SiO_2 is 50nm at an incident angle of 68^0. The Teflon AF-1600 thickness was 500nm.

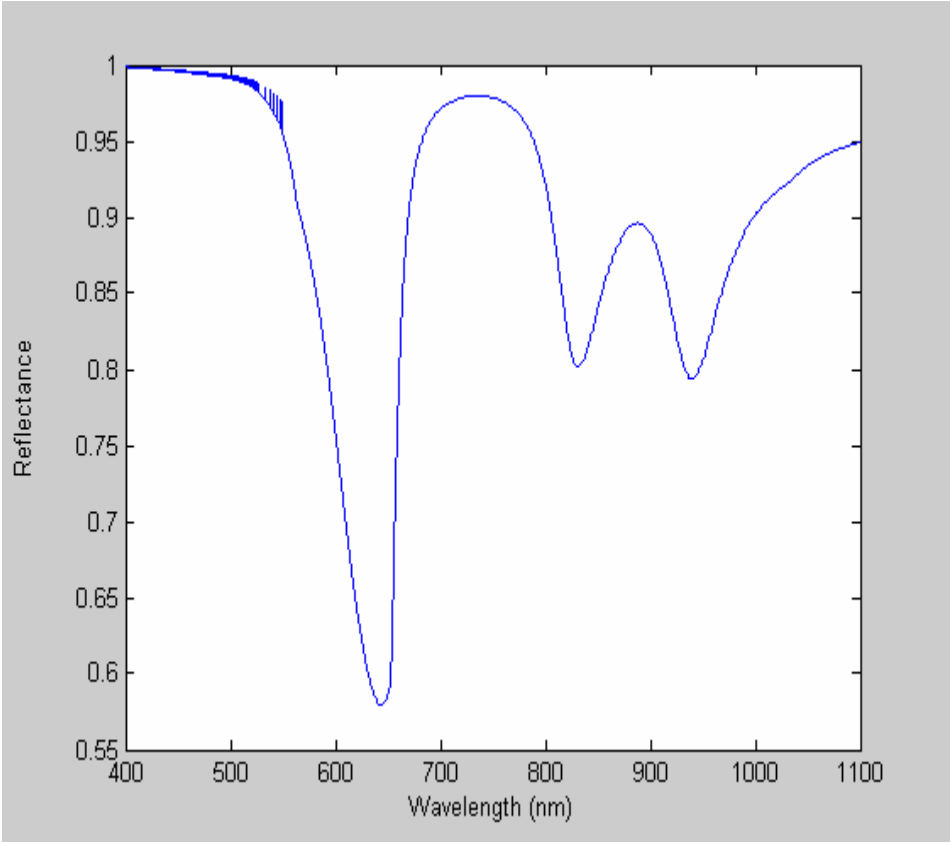

Plot 4.1 Expected Plot when Incident Beam Overlaps Gold and SiO_2 Regions Separately

Since we did not fabricate the device with right thicknesses, we did not get the expected result. However we could measure the reflection spectrum for each of the two surfaces individually. The below figure shows the experimental spectrum obtained from the fabricated sensor.

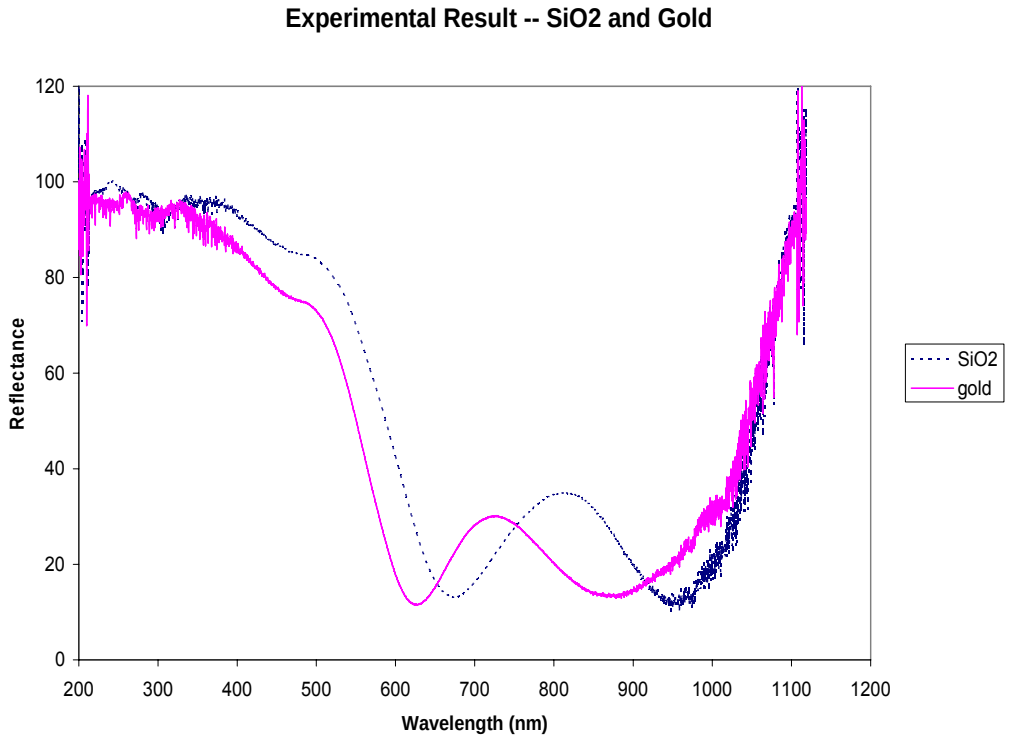

Figure 4.3 Experimental results from the bare gold and gold coated SiO_2 surfaces.

Though the resonance wavelengths didn't match with the simulation results, we could get four distinct dips (two for each region), as shown in the above figure. The simulation spectrum is show below.

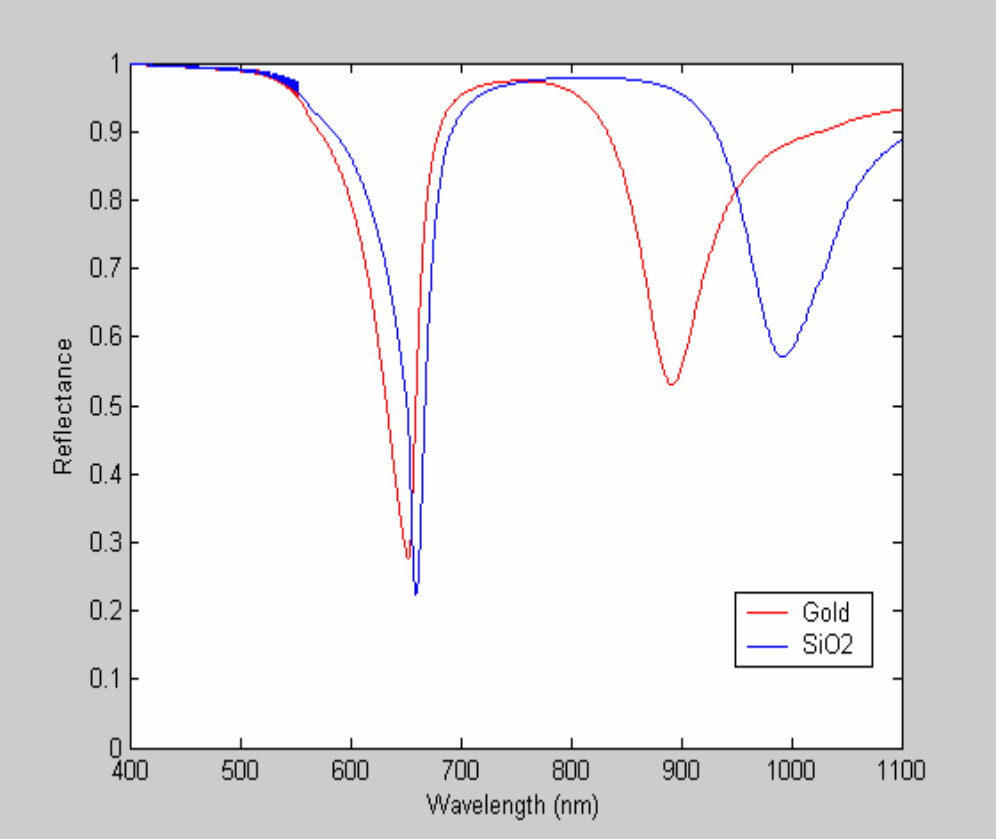

Plot 4.2 Expected Result when light is incident on Gold and SiO_2 regions

4.4 Probable Reasons for Mismatch in the Results

Thickness of each layer plays a huge role in the occurrence of resonance. Variation in thickness of any of the layers can lead to widening the dips or pushing them into the high noise infrared region, making it difficult to measure. A sensor may even cease to behave as self referencing with slight variation in the thicknesses. When the sensor is simulated with gold thickness as 60nm and SiO_2 thickness as 60nm, the spectrum looks very much different from what it was when the thickness were 55nm and 50nm respectively.

.

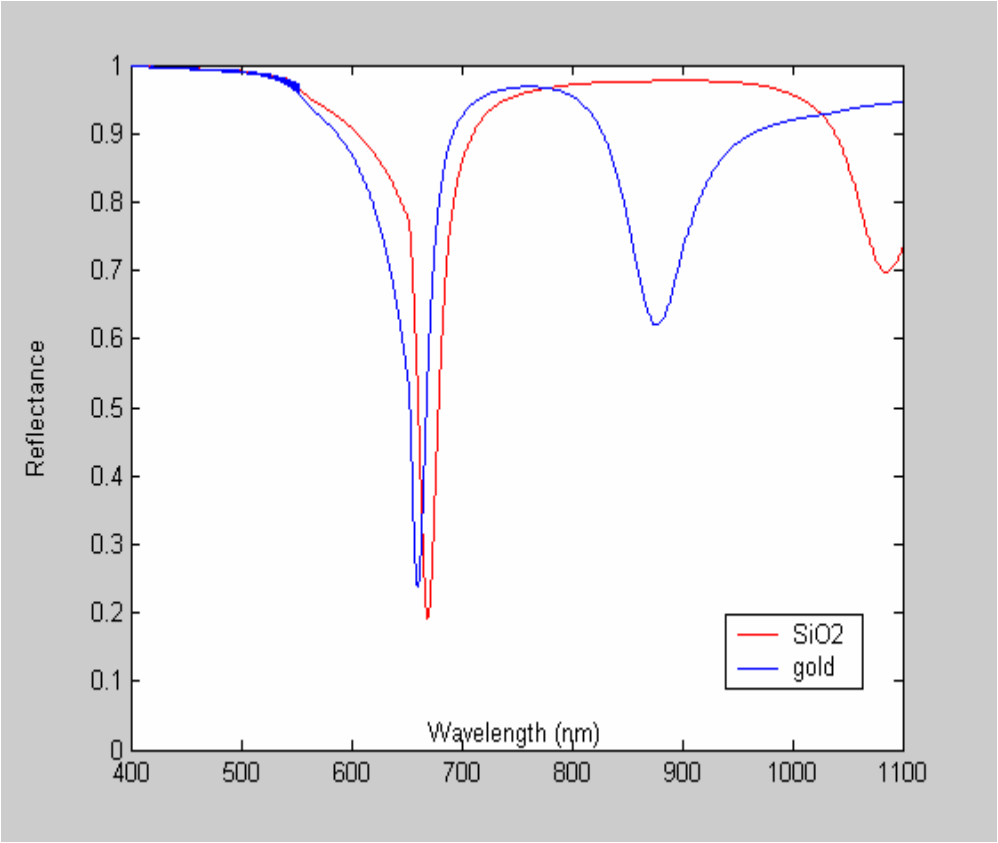

Plot 4.3 Simulated Result when Thickness of SiO_2 = 60nm and Gold = 60nm

The resonance dip for SiO_2 is completely into noise region where it is difficult to measure. Thus because of not get getting the exact thickness values, we couldn't get the expected spectrum.

Another important variant is the angle of incidence. Results change dramatically when there is any slight variation in the angle of incidence. This fact is evident from the following plot. The reflection spectrum for gold is shown in the plot, similar effect was observed for SiO_2 too.

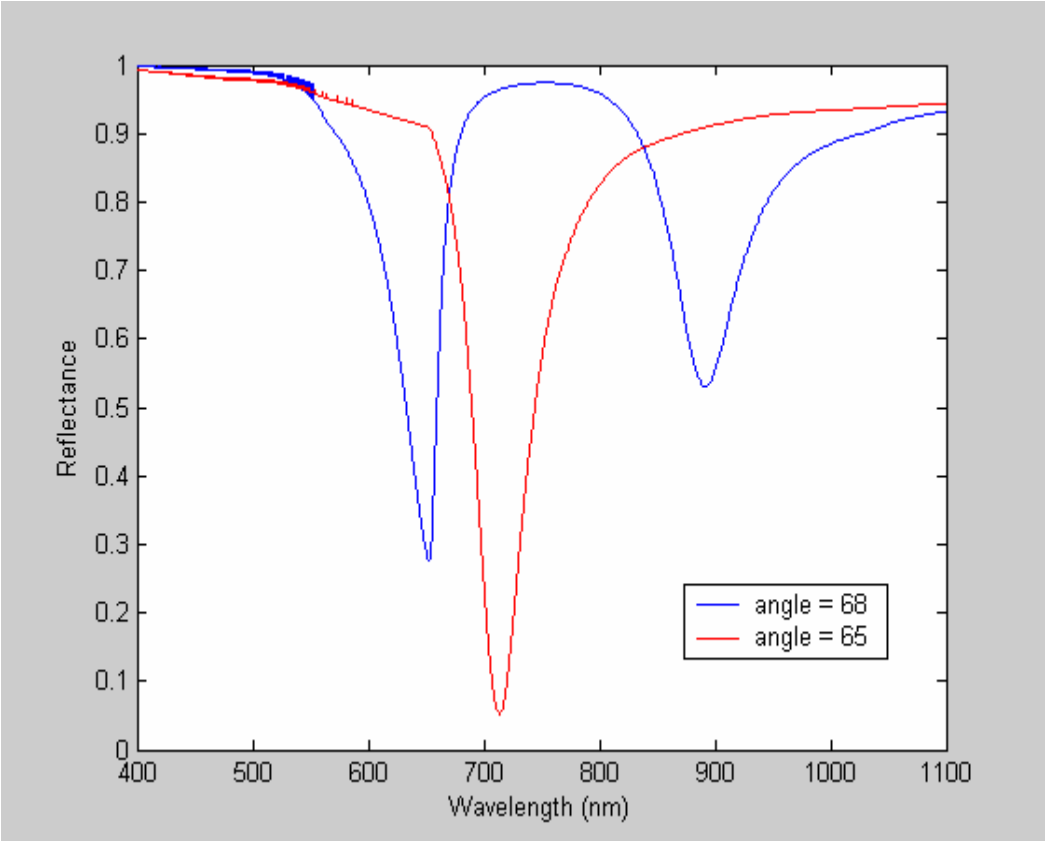

Plot 4.4 Difference in the Reflectance Spectrum of Gold when the angle of incidence is changed to 65^0

As can be seen from the above plot the sensor ceases to behave as self referencing for a change of 3^0 in the angle of incidence. With the right thickness values, we can expect the simulated results as we have obtained four distinct resonance dips, which shows that the two materials behave differently for the refractive index changes.

4.5 Results

The following graphs show the shift in the resonance with the change in the refractive index. We note that the device is not optimized and the short range resonance was in a high noise region as indicated by the plots below.

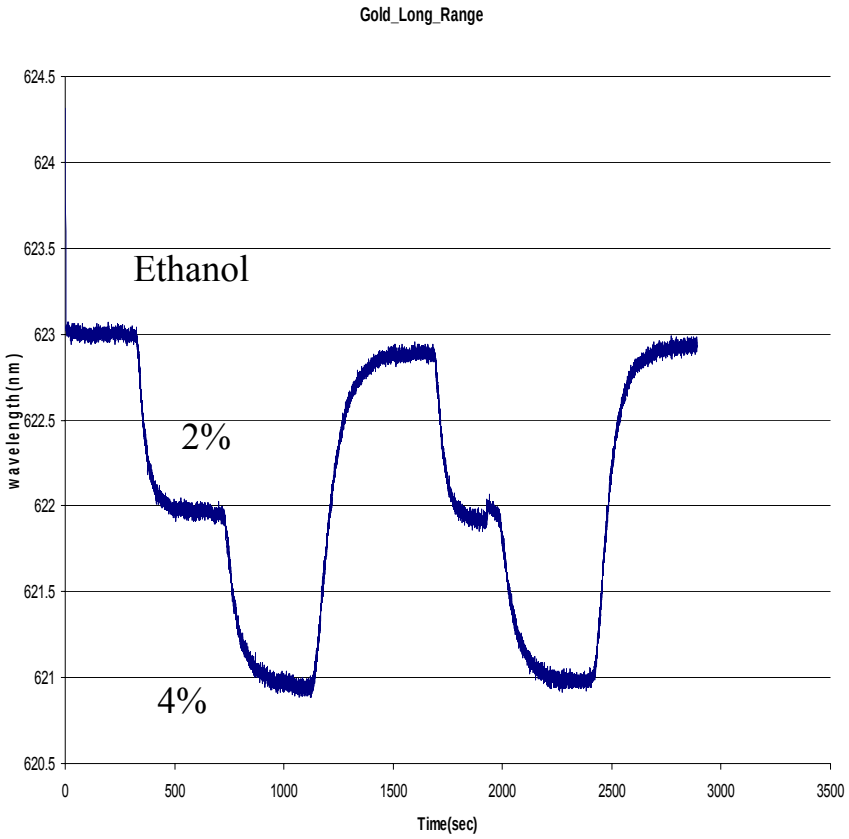

Plot 4.5 Long range surface plasmon resonance wavelength for the bare gold surface when exposed to different concentrations of methanol in ethanol.

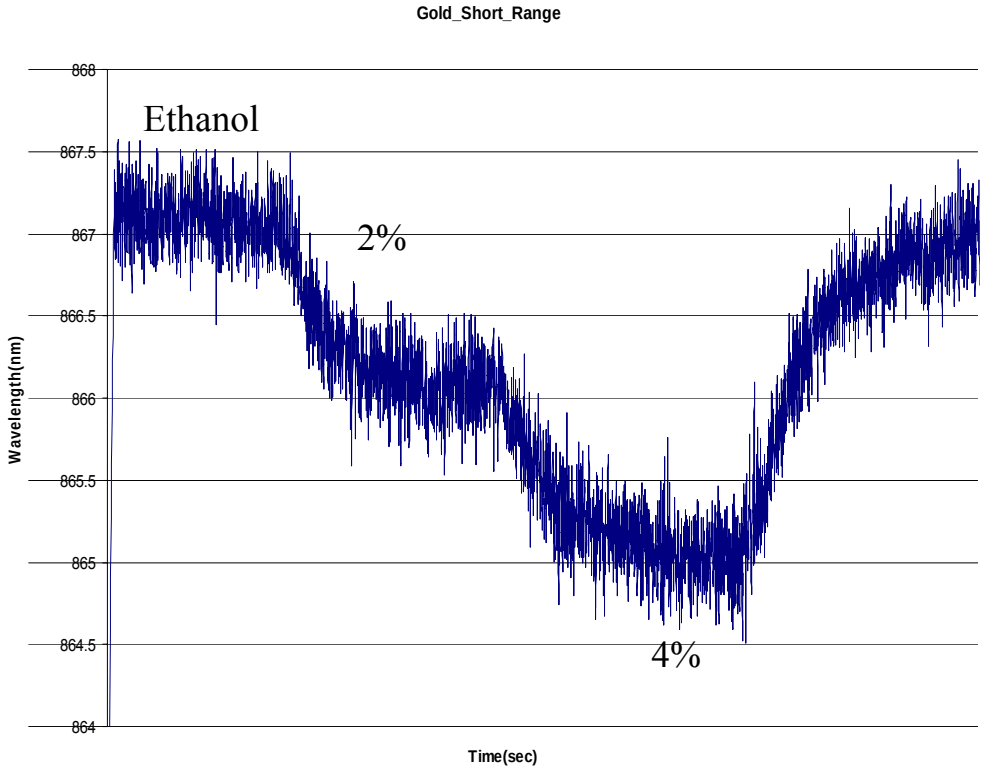

Plot 4.6 Short range surface plasmon resonance wavelength for the bare gold surface when exposed to different concentrations of methanol in ethanol.

The following plots are obtained when the light was incident on the SiO_2

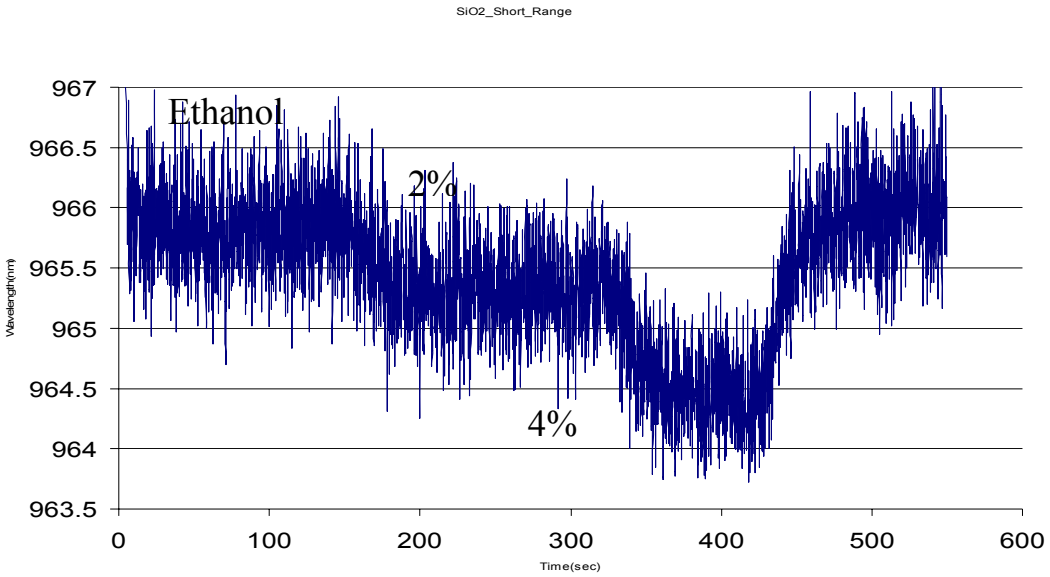

Plot 4.7 Short range surface plasmon resonance wavelength for the SiO_2 coated surface when exposed to different concentrations of methanol in ethanol.

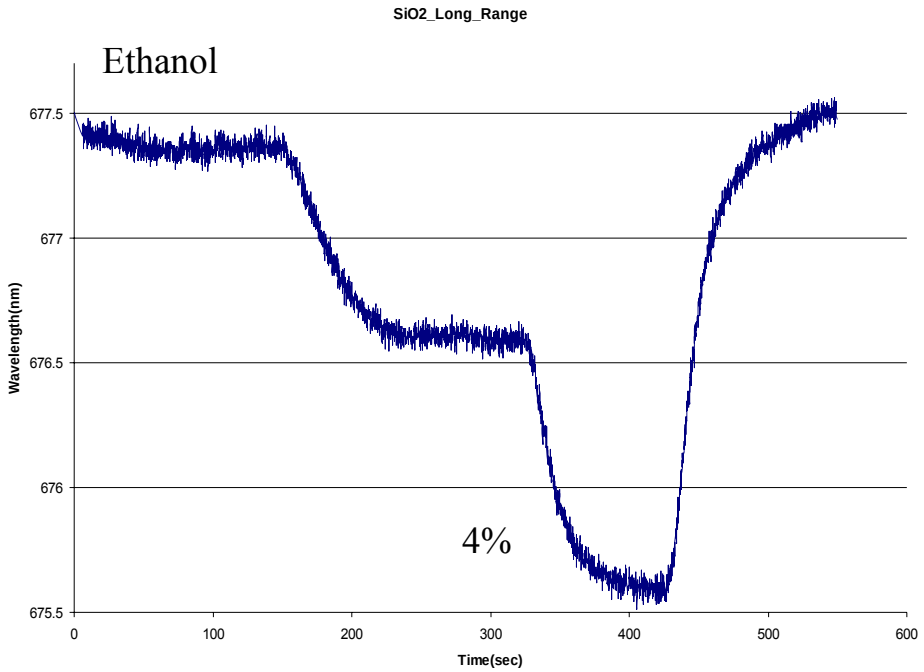

Plot 4.8 Long range surface plasmon resonance wavelength for the SiO_2 coated surface when exposed to different concentrations of methanol in ethanol.

The following plots show the reflectance spectrum when ODT was flowed over the sensor along with other solutions. Note the permanent change in the resonance wavelength after exposure to ODT. This indicates the formation of an ODT monolayer on the gold surface. The high affinity of the thiol molecule for gold makes this binding process essentially irreversible.

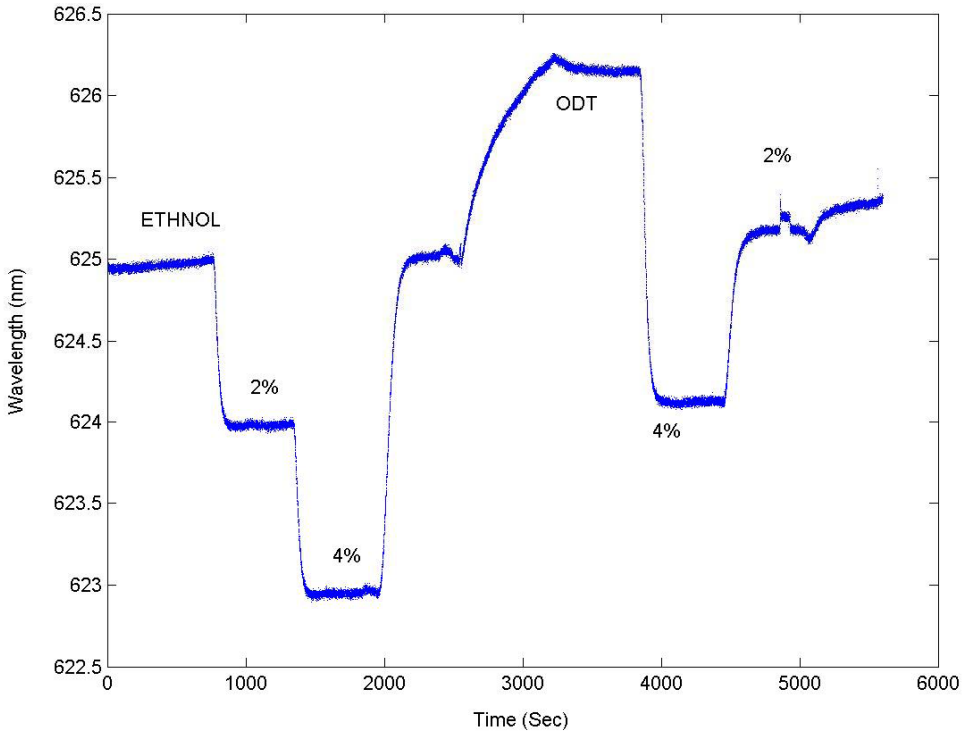

Plot 4.9 Gold_LRSP resonance wavelength when ODT is flowed over the sensor

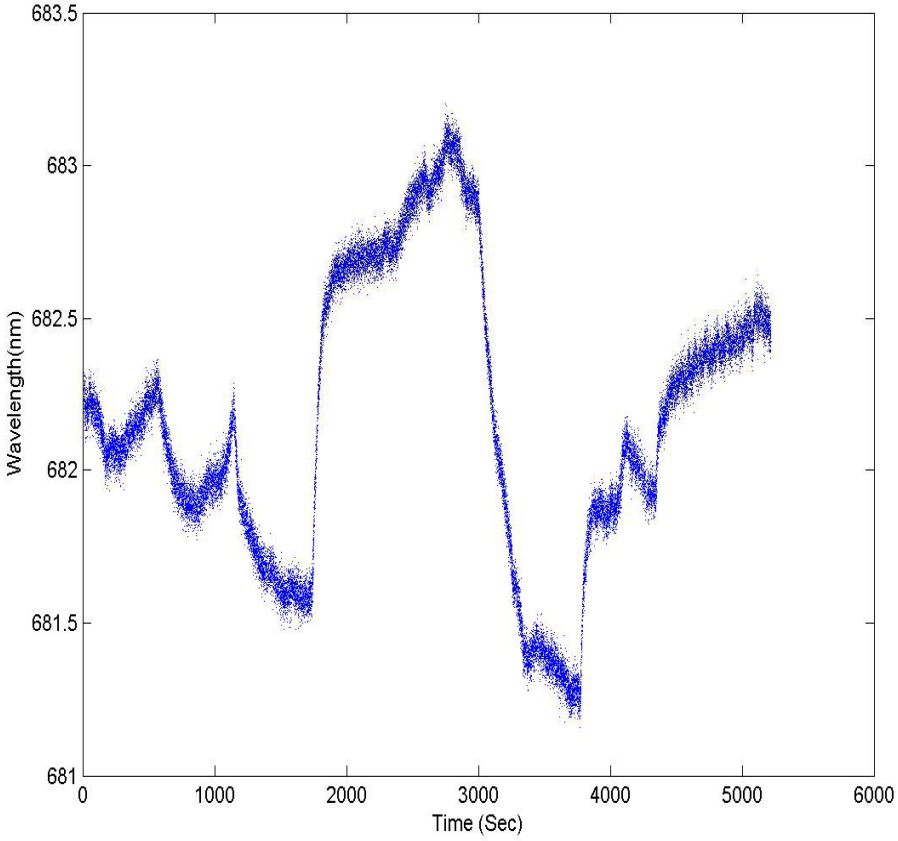

Plot 4.10 SiO2_LRSP when ODT is Flowed over the Sensor

The surface and bulk sensitivities obtained when light beam was incident on gold and SiO_2 are listed below.

Table 4.1 Experimental results

Material	$S_{B\text{-}LR}$ (nm/RIU)	$S_{B\text{-}SR}$ (nm/RIU)
Gold	1811.32	2535.84
SiO_2	1369.05	2245.28

Material	$S_{S\text{-}LR}$ (nm/nm-thickness)	$S_{S\text{-}SR}$ (nm/nm-thickness)
Gold	0.585	2.25
SiO_2	0	0

Chapter 5

FABRICATION CHALLENGES

5.1 Overview

This project was marred with equipment failures and many obstacles in fabrication which took considerable time to get over, major ones being the surface roughness of Teflon AF-1600 and adhesion of PMMA to Teflon AF-1600. In spite of overcoming these issues we couldn't fabricate channel waveguides with Teflon AF-1600 and PMMA using photolithography. This chapter describes our initial design and why it didn't work. During the early stages of the project, channel waveguides with Teflon AF-1600 as cladding and PMMA as core were designed and photolithography was planned to be used for the formation of waveguides on PMMA. A clear description of the fabrication process and where it failed is given below.

5.2 Fabrication of Channel Waveguides

After the regular wafer cleaning, Teflon AF-1600 was spin coated on it at a spin speed of 500 RPM for 12 seconds followed by 1000 RPM for 30 seconds. It was then soft baked for 15 minutes at 185^0C

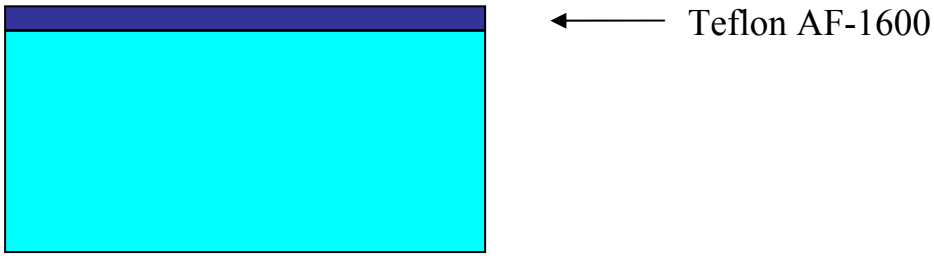

This is followed by oxygen plasma etch for 60 seconds at 50% power. PMMA is then spin coated on the etched Teflon AF-1600 surface at the speed of 1000 RPM and then baked at 180^0C for 5 minutes.

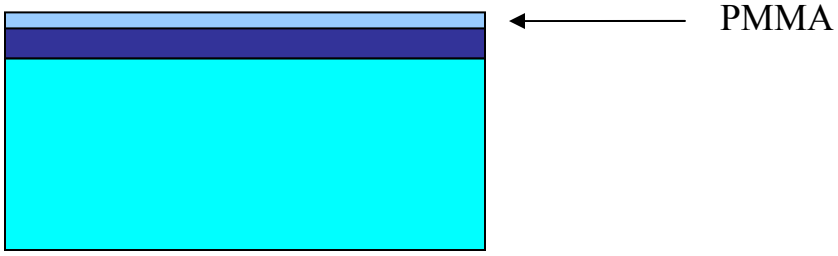

To form waveguides, positive photo resist (Shipley's 1813 resist) is spin coated on the PMMA surface at 400 RPM for 30 seconds and baked at 115^0C for one minute.

The resist is then exposed through the mask for 20 seconds and developed for 30 seconds in positive resist developer MF-319 developer (Microposit).

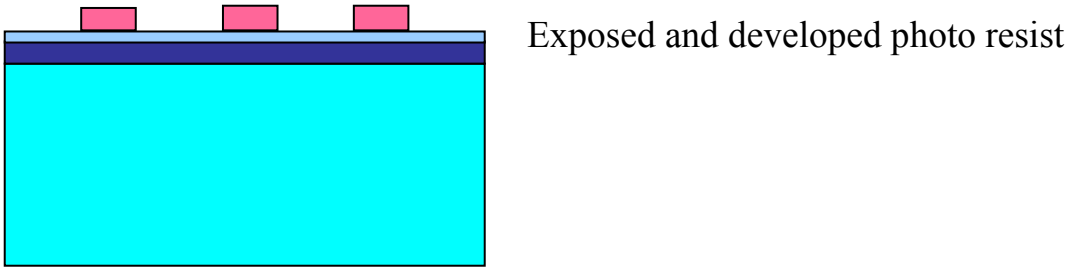

The remaining resist is again exposed without the mask such that all the remaining photo resist is also exposed.

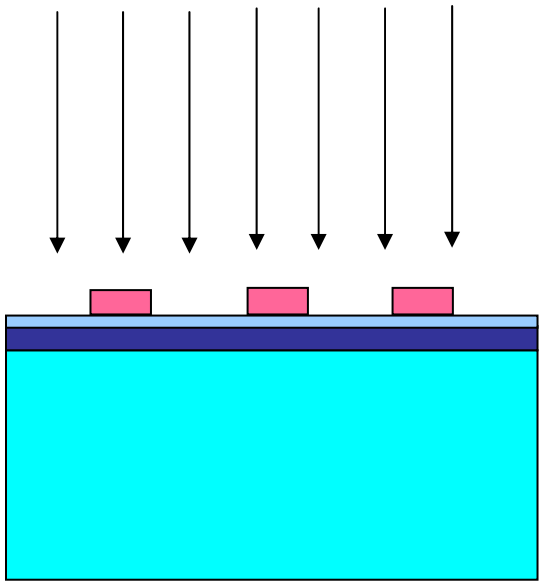

On the exposed resist, 30nm of SiO_2 was deposited in e-beam evaporator.

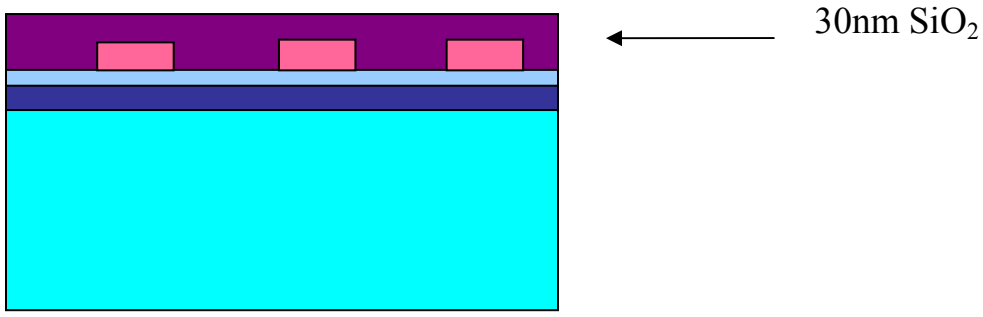

The wafer is then immersed in the positive resist developer so that the SiO_2 is lifted off along with the exposed resist. We couldn't get the lift off to happen even after leaving the wafer in the developer overnight. We increased second exposure time to 90 seconds and repeated experiment, but didn't achieve any success. Below are described further steps had the lift off been a success. Assuming that the SiO_2 was lifted off:

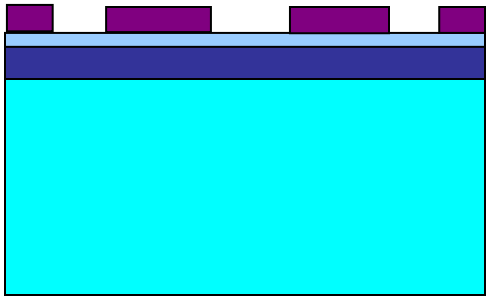

After lift off

The wafer would be plasma etched for 15 seconds at 10% power so that exposed PMMA is removed. Thus SiO_2 acts as a mask.

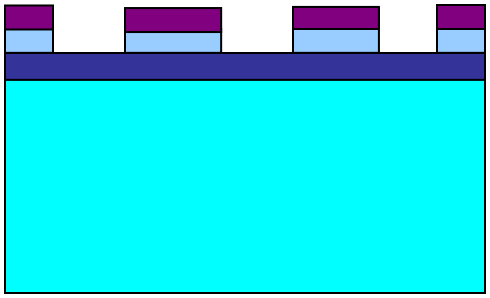

After Oxygen Etch

Then SiO_2 would be removed in hydrofluoric acid (HF) and finally we would get PMMA channel waveguides on Teflon AF-1600 surface.

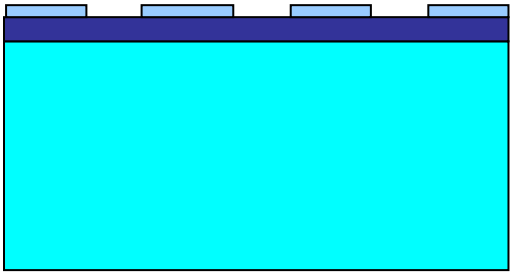

PMMA channels

Teflon AF-1600 should be again spin coated on PMMA as upper cladding.

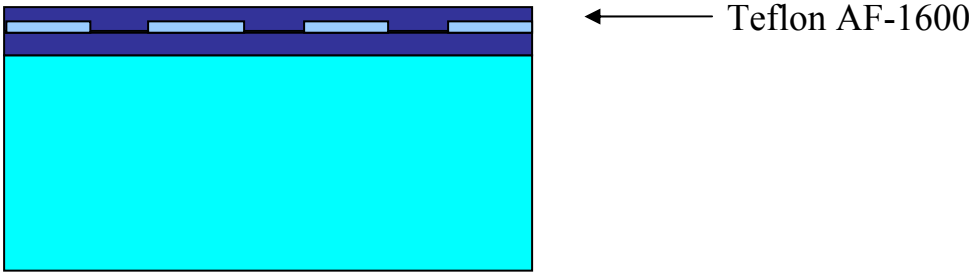

Chapter 6

CONCLUSIONS AND FURTHER WORK

6.1 Possible Variations in the Design

We expect that varying the thicknesses of various layers of the sensor will yield experimental spectra similar to the simulated results. Making the SiO_2 layer thinner will move the SRSP resonance to shorter wavelengths making it possible to measure the resonance dip. Also making the Teflon thinner will make the resonance dips of gold and SiO_2 more distinguishable. However, changing the gold thickness will have no positive effect. Making the gold thicker will cause the SRSP and LRSP to overlap. Making the gold thinner will cause the SRSP associated with the gold to overlap the one corresponding to the SiO_2. In addition, making the gold thinner beyond a certain value will place the SRSP resonance outside the wavelength range of the spectrometer and prevent self referencing.

6.2 Conclusions

The choice of right kind of solvent for Teflon AF-1600 is the first step to fabricate any device as Teflon AF-1600 layer can be unacceptably rough depending on the solvent. Other key lesson learned in the fabrication process was that the Teflon AF-1600 surface needs to be altered in order to make other polymers adhere to it. This possibility opens many doors to myriad combinations with which devices can be

designed as Teflon AF-1600 is one of the few low refractive index solids. These two factors hold the key to fabrication of any Teflon AF-1600 – PMMA based optical device.

In case of SPR sensors, thicknesses control their proper functioning. Slight differences in the thickness of gold and silicon dioxide can alter the reflectance spectra dramatically. Unfortunately, with no means to measure the thickness values of any of the three involved materials, we had to use our best guess in the fabrication of SPR sensors. The crystal monitor on the e-beam evaporator was found to be highly erroneous as obtained results were no where close to the simulated results obtained using crystal monitor readings. Fabricating a sensor with the specified gold and SiO_2 thicknesses should yield a greater difference in the sensitivities of LRSP and SRSP to solution index changes. In addition, the measurement of four different resonances (LRSP and SRSP with and without and SiO_2 overlayer) suggests that we can build a self-referencing sensor that compensates for both solution index changes and for non-specific binding.

6.3 Suggestions for Further Work

The first critical step towards fabricating a working device is to have highly precise measurements of thickness values. Samples at various stages of the fabrication process could be sent off to be measured or taken to a collaborative institution with the appropriate equipment to give accurate thickness values. If the sensor could be fabricated according the specified thickness values, one can hopefully obtain results matching the simulations. The challenge will be to optimize the device such that all the resonances lay well within the low noise measurement regions or to provide a supplemental infrared light source.

Waveguides with integrated Bragg gratings could be written using the EBL system as the patterns and a known fabrication process is well in place. In line with our original plan, PMMA could be replaced with dye-doped PMMA to produce electro optical polymer waveguide devices. However this would require re-designing few details according to the refractive index of the dye-doped PMMA.

REFERENCES

1. Cherin, Allen.H, *An Introduction to Optical Fibers*, New York: Mc Graw-Hill, c1983

2. Hong.Ma, Alex K-Y.Jen, Larry R. Dalton, *Polymer-Based Optical Waveguides Materials, Processing and Devices.* Advance Materials, 2002. **14**(19): p.1339-1365.

3. Anadi Mukherjee, Ben Joy Eapen, and Swapan K.Baral, *Very low loss channel waveguides in polymethylmethacrylate*. Applied Physics Letters, 1994. **65**(25): p.3179-3181.

4. W.H.Wong and E.Y.B.Pun, *Polymer waveguide wavelength filters using electron-beam direct writing*. American Institute of Physics, 2001. **79**(22): p.3576-3578

5. Y.-G.Zhao, W.-K.Lu, Y.Ma, S.-S.Kim, and S.T.Ho, *Ploymer waveguides useful over a very wide wavelength range from the ultraviolet to infrared.* American Institute of Physics, 2000. **77**(19): p.2961-2963

6. Hastings, J.T., R. Donipudi, and V. de Silva, *Self-referencing SPR Sensors using both Long- and Short-Range Surface-Plasmons.* Submitted to Sensors and Actuators B-Chemical, 2005.

7. Homola, J., S.S. Yee, and G. Gauglitz, *Surface plasmon resonance sensors: review.* Sensors and Actuators B-Chemical, 1999. **54**(1-2): p. 3-15.

8. Nenninger, G.G., et al., *Long-range surface plasmons for high-resolution surface plasmon resonance sensors.* Sensors and Actuators B-Chemical, 2001. **74**(1-3): p. 145-151.

9. Albuquerque, L., C. Ventura, and R. Goncalves, *Refractive indices, densities, and excess properties for binary mixtures containing methanol, ethanol, 1,2-ethanediol, and 2-methoxyethanol.* Journal of Chemical and Engineering Data, 1996. **41**(4): p. 685-688

10. Bain, C.D., et al., *Formation of Monolayer Films by the Spontaneous Assembly of Organic Thiols from Solution onto Gold.* Journal of the American Chemical Society, 1989. **111**(1): p. 321-335.

11. Boozer, C., et al., *Surface functionalization for self-referencing surface plasmon resonance (SPR) biosensors by multi-step self-assembly.* Sensors and Actuators B-Chemical, 2003. **90**(1-3): p. 22-30.

12. Hastings, J.T., *Nanometer-Precision Electron-Beam Lithography with Applications in Integrated Optics, 2003*.

13. Lowry, J.H., J.S. Mendlowitz, and N.S. Subramanian, *Optical Characteristics of Teflon Af(R) Fluoroplastic Materials.* Optical Engineering, 1992. **31**(9): p. 1982-1985.

VITA

The author was born in Vijayawada, Andhra Pradesh, India on February 7, 1981. In 1993, she completed her under graduation in India at Nagarjuna University, in the Department of Electrical Engineering. In August 2003 she was awarded Kentucky Graduate Scholarship and joined University Of Kentucky to pursue her MS in Electrical Engineering. During the course of the program, she worked in the Department of Electrical Engineering as a Teaching Assistant and as a Research Assistant at Centre for Nanoscale Science and Engineering (CeNSE).